

Topics in Boundary Quantum Field Theory

Magnetic Edge States in Graphene and BCFT Orbifold

by

Shovon Biswas

B.Sc., Bangladesh University of Engineering and Technology, 2018

A THESIS SUBMITTED IN PARTIAL FULFILLMENT OF
THE REQUIREMENTS FOR THE DEGREE OF

MASTER OF SCIENCE

in

The Faculty of Graduate and Postdoctoral Studies

(Physics)

THE UNIVERSITY OF BRITISH COLUMBIA

(Vancouver)

August 2021

© Shovon Biswas 2021

The following individuals certify that they have read, and recommend to the Faculty of Graduate and Postdoctoral Studies for acceptance, the thesis entitled:

Topics in Boundary Quantum Field Theory: Magnetic Edge States in Graphene and BCFT Orbifold

submitted by **Shovon Biswas** in partial fulfillment of the requirements for the degree of MASTER OF SCIENCE in PHYSICS.

Examining Committee:

Gordon W. Semenoff, Professor, Physics and Astronomy, UBC
Supervisor

Joanna L. Karczmarek, Associate Professor, Physics and Astronomy, UBC
Supervisory Committee Member

Abstract

In this thesis, we investigate two examples of quantum field theory with planar boundaries. In the first part, we study the low energy excitations in a semi-infinite graphene sheet with the zigzag boundary condition. The system is described by a massless Dirac field with boundary condition such that half of the spinor components vanish on the boundary. From the residual continuous and discrete symmetries of the system, we argue that the graphene zigzag edge should be ferromagnetic. In the second part, we study symmetric orbifold boundary conformal field theory (BCFT). We show how to construct Cardy consistent boundary states for this symmetric orbifold BCFT. We also compute the boundary entropy and comment on its relevance to the AdS/BCFT correspondence.

Lay Summary

In the first part of this thesis, the physics of graphene, a two-dimensional material made of carbon, is studied. It is argued that when cut in a particular way, the graphene edge can be magnetic.

Quantum gravity is a theory that aims to describe the strong effects of gravity such as the physics inside a black hole. In the second part of the thesis, a theory called “Symmetric product boundary conformal theory” is constructed. This theory is used to explore some ideas in quantum gravity.

Preface

Section 2.3 includes original, unpublished results. The project was proposed by Gordon Semenoff. I completed various calculations that helped formalize the main result of the section.

Section 4.3 includes original, yet unpublished work done in collaboration with James Sully and Alexandre Belin. The project was proposed by James Sully and I performed various calculations that revealed the general structure of boundary states for various example cases, finally resulting in the main formula of boundary states. A manuscript based on the main result of this section is under preparation.

Table of Contents

Abstract	iii
Lay Summary	iv
Preface	v
Table of Contents	vi
List of Figures	viii
Acknowledgements	ix
Dedication	x
1 Introduction	1
2 Symmetries and Their Consequences	3
2.1 Symmetry and conserved charge	4
2.2 Emergent Relativistic Symmetry in Graphene	8
2.3 Ferromagnetic Edge State in Graphene	12
3 Conformal Field theory	20
3.1 Conformal transformations in d dimensions	20
3.2 CFT in $d = 2$ dimensions	21
3.2.1 Virasoro Algebra	23
3.2.2 The Hilbert Space	29
3.2.3 Torus Partition Function	30
3.3 Boundary Conformal Field Theory	34
3.3.1 The Doubling Trick	34
3.3.2 Cardy's Condition	36

Table of Contents

4	Symmetric Orbifold BCFT	40
4.1	AdS/CFT Correspondence and Symmetric Orbifold	40
4.2	AdS/BCFT Correspondence	42
4.3	Boundary States in Symmetric Orbifold BCFT	44
4.3.1	Ansatz for Boundary State	44
4.3.2	Example 1: $N = 2$	45
4.3.3	Example 2: $N = 3$	46
4.3.4	Boundary Entropy and Brane Spectrum	48
5	Conclusion	51
	Bibliography	52
A	Useful Relations in Complex Coordinates	56

List of Figures

2.1	a) The hexagonal lattice structure of graphene is comprised of two inequivalent sublattice atoms, denoted here by A and B. b) A choice of basis vector for the A sublattice. Acting on by $m\vec{a}_1 + n\vec{a}_2$ with m, n integers, it is possible to move around between all A points.	9
2.2	Two inequivalent ways of cutting the graphene sheet	13
3.1	In the cylinder time runs along the length of the cylinder and the space direction is compactified in a circle. The cylinder is mapped to the complex plane by mapping $z = e^w$, $w = x^0 + ix^1$	23
3.2	The integration contour of eq. (3.21) can be deformed into a contour tightly wound around w	26
3.3	Torus in the complex plane whose periods are chosen to be 1 and τ	31
3.4	Using the doubling trick, the theory in the upper half plane can be mapped to a theory defined on the full plane.	35
3.5	Using doubling trick the semi-circular integration contours in upper half plane can be deformed to a circular contour in full plane. On the real line the contributions from each semi-circle cancel due to (3.51).	35
3.6	With a periodic trajectory in σ^0 direction, the infinite strip becomes a cylinder with boundary conditions a and b on each side.	36
4.1	The CFT is defined on a manifold M with boundary ∂M . On the bulk the boundary ∂M extends to the boundary Q of the dual N of M such that $\partial N = M \cup Q$	42
4.2	The gravity dual of half line. The location of the boundary $\rho = \rho^*$ depends on the brane tension via (4.8) and $\cot \theta = \sinh \frac{\rho^*}{l_{AdS}}$	43

Acknowledgements

I would like to thank my supervisors Gordon W. Semenoff and Joanna Karczmarek for their support and inspiration in every way possible. Professor Semenoff's adroitness in every branch of physics has always been very inspiring for me. Whenever I was stuck with something, Professor Karczmarek's crystal clear explanations rescued me. I also express my gratitude to both of them for supporting my mental health throughout the difficult time of the pandemic. To my knowledge, such instances are rare in academia.

My special thanks to James Sully for acting as honorary supervisor during my degree. He has always been very kind in patiently answering all my questions over the past two years and guiding me. Thanks to Alex Belin for his collaboration on the project.

I would like to thank my undergraduate supervisors Arshad Momen and Zunaid Baten. Without them, the transition from electrical engineering to theoretical physics would have been impossible. In particular, without Professor Arshad Momen, this journey would have never started.

I would like to express my gratitude to all members of the UBC string theory group. In particular, many thanks to Petar Simidzija and David Wakeham for their support, friendship, (and for listening to my rants). Special thanks to Jonnah Berean-Dutcher and Tomasz Andrzejewski for pandemic hangouts that kept me sane.

Finally but most importantly, all credit goes to my family and friends. Their constant support and encouragement fuel me every single day. This thesis would be impossible without support and love from Anya, Anu, Rafid, Pritam, Tahsin, and Rahgeer. You guys know how much you matter to me.

Dedication

To my parents and sister.

Chapter 1

Introduction

Quantum field theories are the key tools in theoretical high-energy physics in explaining nature. Numerous predictions of QFT have been explicitly verified in particle colliders over the past few decades. In the standard QFT literature, the role of physical boundaries is trivialized by imposing various boundary conditions on the fields. However, there are instances when the presence of a boundary of the system under investigation cannot be ignored. Indeed, infinite systems are just mathematical idealizations and all measurable physical systems are finite. In fact, in many cases, boundary physics is much richer than bulk physics. A few examples are the Kondo effect in condensed matter, D-branes in string theory, etc.

Motivated by these examples, in this thesis we investigate two instances of boundary quantum field theories. In the first part, we apply our theoretical tools to study a semi-infinite graphene sheet. The physics of graphene can be described by the relativistic Dirac equation in $2 + 1$ dimensions. There is a particular way of cutting the graphene sheet known as the zigzag boundary. We show how to realize this boundary condition in the language of quantum field theory. Finally, we argue that the zigzag edge of graphene is ferromagnetic.

In the second part, we study a special boundary quantum field theory called the boundary conformal field theory (BCFT). BCFTs in two dimensions are well studied in the context of surface critical phenomena in statistical mechanics. We study a special type of BCFT called symmetric product orbifold BCFT. Symmetric product orbifold CFTs (i.e. without a boundary) has been studied extensively in the context of string theory [10] and the AdS/CFT correspondence [1, 2, 21]. However, a similar investigation for BCFTs has not been done yet. In particular, we discuss how to construct Cardy consistent boundary states in symmetric product BCFT. In the large N limit, where N

denotes the number of copies in the symmetric orbifold, our analysis reveals the spectrum of constant-tension branes in AdS/BCFT correspondence.

The organization of the rest of the thesis is as follows: in chapter 2, we discuss the emergence of ferromagnetism in semi-infinite graphene sheet with zigzag boundary. In chapter 3, we discuss the basics of conformal field theory and boundary conformal field theory, and finally, in chapter 4, we discuss the symmetric product orbifold BCFT.

Chapter 2

Symmetries and Their Consequences

In many physical systems, symmetries are often emergent. A simple example is a crystal with lattice spacing a . Continuous translations and rotations are *not* symmetries of this system. However, if we observe the system at a length scale $l \gg a$, i.e from very ‘far’, the system looks continuous. In this $l \gg a$ limit, we say that continuous translation and rotation are emergent symmetries of the system. In physics, there are many examples where the low energy degrees of a condensed matter or statistical systems can be described by a Quantum Field Theory (QFT). As an example, we shall discuss in section 2.2 how the low energy physics of graphene can be described by a fermionic QFT.

In addition to translation and rotation, there are instances when a system exhibits emergent scaling symmetry. When it happens, the system gains the property that if all lengths are multiplied by a constant factor, the physics remains unchanged. A canonical example of this phenomenon is a system near the second-order phase transition. In general, the correlation between two points of the system decays like $\sim e^{-r/\zeta}$, where ζ is a characteristic length scale known as the correlation length and r is the distance between the points. When the system undergoes the phase transition, ζ diverges. This signals that all points of the system become strongly correlated with each other. At this instant, the system becomes scale-invariant. More specifically, if we say that our system undergoes a phase transition as we tune the temperature T of the system, ζ is a function of T . If the phase transition occurs at T_c , near this value $\zeta \sim \frac{1}{T-T_c}$. So as we tune the temperature T of the system, scale symmetry emerges when $T \sim T_c$.

For a large number of systems, Poincare+Scale symmetry implies that the system has a more enhanced symmetry structure known as

conformal symmetry. A very frivolous example is a massless free field theory. Since the mass is zero, there is no natural scale of the system and it can be explicitly checked that the theory has conformal symmetry. However, in this chapter, we will find that putting a physical boundary in such systems might have very non-trivial consequences. As mentioned before, the physics of low-energy modes of graphene is described by massless free fermionic QFT. As a result, it should have conformal symmetry. We shall see that cutting it by half in a specific way i.e putting a boundary severely alternates the system structure. In particular, we shall use continuous and discrete symmetry to argue that the edge of a semi-infinite graphene sheet with a zigzag boundary should be ferromagnetic. The organization of the chapter is as follows: in section 2.1 we review some standard topics in QFT, next we will review how graphene can be described by the massless free Dirac in section (2.2). Finally, in section (2.3), we will present our argument for the ferromagnetic edge state.

2.1 Symmetry and conserved charge

The basic objects in QFT are quantum fields. They can be of scalar, tensor or spinor valued. The first task in QFT is to construct an action of the form

$$S = \int d^d x \mathcal{L}(\Phi(x), \partial_\mu \Phi(x)) \quad (2.1)$$

having the following properties

- The action is consistent with the Poincare symmetries and
- It is “local”.

Our center of interest in this thesis will be symmetries. Let us definite what we mean by that.

Definition 1. *Consider a transformation of the field $\Phi \rightarrow \Phi'$. The transformation is called a symmetry transformation if the transformed field Φ' also satisfies the same equation of motion as the original field Φ .*

In particular this ensures that the action remains unchanged i.e.

2.1. Symmetry and conserved charge

Corollary 1. *Under a symmetry transformation $\Phi \rightarrow \Phi'$ the change in action $\delta S = 0$.*

Consider the infinitesimal change $\delta\Phi = \Phi(x) - \Phi'(x)$ as a result of a symmetry transformation. The change in the action is given by

$$\begin{aligned}\delta S &= \int d^d x \left[\frac{\partial \mathcal{L}}{\partial \Phi} \delta\Phi + \frac{\partial \mathcal{L}}{\partial \mu \Phi} \delta(\partial_\mu \Phi) \right] \\ &= \int d^d x \left[\frac{\partial \mathcal{L}}{\partial \Phi} - \partial_\mu \left(\frac{\partial \mathcal{L}}{\partial \mu \Phi} \right) \right] \delta\Phi + \int d^d x \partial_\mu \left(\frac{\partial \mathcal{L}}{\partial \mu \Phi} \delta\Phi \right)\end{aligned}\quad (2.2)$$

On classical solution i.e when the fields satisfy the classical equation of motion, the term inside the square parenthesis vanishes. Since the transformation is a symmetry, the change in action must be $\delta S = 0$. This is true as long as the second term is equal to some total derivative, say $\partial_\mu X^\mu$. Thus, we have for a symmetry transformation

$$\delta S = \int d^d x \partial_\mu \left(\frac{\partial \mathcal{L}}{\partial \mu \Phi} \delta\Phi - X^\mu \right) = 0. \quad (2.3)$$

The quantity

$$J^\mu \equiv \frac{\partial \mathcal{L}}{\partial \mu \Phi} \delta\Phi - X^\mu \quad (2.4)$$

is called **Noether current**. When evaluated on the classical solution, Noether current satisfies

$$\partial_\mu j^\mu = 0. \quad (2.5)$$

This enables us to define the **Noether charge**

$$Q \equiv \int d^{d-1} x J^0(x) \quad (2.6)$$

Using (2.5) it is easy to show that if the spatial components $j^i(x)$ vanish at the boundary of the manifold, then $\frac{d}{dt} Q = 0$.

To illustrate the ideas, let us discuss the symmetries of the massless free Dirac field. We shall see that this simple theory has a rich symmetry structure. This will also be our first example of a system with conformal symmetry.

2.1. Symmetry and conserved charge

The massless free Dirac theory is described by the following action:

$$S = \int d^d x \mathcal{L}(x)$$

$$\mathcal{L}(x) = -\frac{i}{2} \bar{\psi}(x) \left(\overleftarrow{\not{\partial}} - \overrightarrow{\not{\partial}} \right) \psi(x). \quad (2.7)$$

In this equation, $\psi^\alpha(x)$ is a $2^{\lfloor d/2 \rfloor \times 1}$ complex-valued column vector that describe a spin- $\frac{1}{2}$ particle in d spacetime dimensions. $\gamma_{\alpha\beta}^\mu, \mu = 0, 1, 2, \dots, d-1$ are $2^{\lfloor d/2 \rfloor} \times 2^{\lfloor d/2 \rfloor}$ matrices that act on the components of $\psi^\alpha(x)$. The spinor indices of both $\psi(x)$ and γ^μ are usually kept implicit. $\bar{\psi}(x)$ is a $1 \times 2^{\lfloor d/2 \rfloor}$ row vector defined as $\bar{\psi}(x) = \psi^\dagger(x) \gamma^0$. The gamma matrices anti-commute

$$\gamma^\mu \gamma^\nu + \gamma^\nu \gamma^\mu = 2\eta^{\mu\nu}. \quad (2.8)$$

The notation \not{A} stands for $\gamma^\mu A_\mu$. Upon quantization, Dirac spinors obey the *equal-time* anticommutation relations

$$\{\psi^\dagger(x), \psi(x')\} = i\delta(x-x'), \quad \{\psi^\dagger(x), \psi^\dagger(x')\} = 0 = \{\psi(x), \psi(x')\}. \quad (2.9)$$

The action (2.7) leads to the following equation of motion for the spinor field

$$\not{\partial}\psi(x) = 0. \quad (2.10)$$

Let's investigate the symmetry contents of the theory. The transformation $\psi'(x) = e^{i\theta} \psi(x)$, $\theta = \text{const.}$ is obviously a symmetry of the Dirac action. Using the infinitesimal form of this symmetry in our formula, we obtain the Noether current

$$J^\mu(x) = \bar{\psi}(x) \gamma^\mu \psi(x). \quad (2.11)$$

This is known as phase symmetry. The corresponding Noether charge is

$$N = \int d^{d-1}x \psi^\dagger(x) \psi(x), \quad (2.12)$$

which is just the total number of particles.

Now let us concentrate on the spacetime symmetry of the free Dirac action

$$x^\mu \rightarrow x'^\mu = x^\mu + f^\mu. \quad (2.13)$$

2.1. Symmetry and conserved charge

Consider a general transformation of the fields under the coordinate change

$$\begin{aligned}\delta_f \psi(x) &= \left(f^\mu \partial_\mu + \Sigma^{\mu\nu} \partial_\mu f_\nu + \frac{\Delta}{d} \partial_\mu f^\mu \right) \psi(x) \\ \delta_f \bar{\psi}(x) &= \bar{\psi}(x) \left(f^\mu \overleftarrow{\partial}_\mu - \Sigma^{\mu\nu} \partial_\mu f_\nu + \frac{\Delta}{d} \partial_\mu f^\mu \right).\end{aligned}\quad (2.14)$$

Here, $\Delta = \frac{d-1}{2}$ and $\Sigma^{\mu\nu} = \frac{1}{8} [\gamma^\mu, \gamma^\nu]$.

Under this transformation the change in the Lagrangian density can be computed to be

$$\delta_f \mathcal{L} = \partial_\mu (f^\mu \mathcal{L}) + \frac{i}{4} \bar{\psi} \left(\overleftarrow{\partial}^\mu - \overrightarrow{\partial}^\mu \right) \gamma^\nu \psi \left(\partial_\mu f_\nu + \partial_\nu f_\mu - \frac{2}{d} \eta_{\mu\nu} (\partial \cdot f) \right) \quad (2.15)$$

Here, we have not used the equation of motion yet. Clearly, if f^μ satisfies

$$\partial_\mu f_\nu + \partial_\nu f_\mu - \frac{2}{d} \eta_{\mu\nu} (\partial \cdot f) = 0, \quad (2.16)$$

the Lagrangian density changes by a total derivative and the transformation (2.13) is a symmetry of the theory. Equation (2.16) is called the **conformal killing equation** and the $f^\mu(x)$ that satisfy (2.16) are called **conformal killing vectors**. The solutions to (2.16) are

$$\begin{aligned}f^\mu &= a^\mu && \text{(Translation)} \\ f^\mu &= \omega^{\mu\nu} x_\nu && \text{(Rotation)} \\ f^\mu &= \lambda x^\mu && \text{(Scaling)} \\ f^\mu &= x^\mu (b \cdot x) - \frac{1}{2} b^\mu x^2 && \text{(Special conformal transformation),}\end{aligned}$$

where λ, a^μ, b^μ are constants and $\omega^{\mu\nu} = -\omega^{\nu\mu}$.

On the classical solution the corresponding Noether charges are given by

$$\mathcal{Q}_f = -\frac{i}{2} \int d^{d-1}x \left(\psi^\dagger(x) \delta_f \psi(x) - \delta_f \psi^\dagger(x) \psi(x) \right) \quad (2.17)$$

where the transformation of the spinors is given in (2.14). Noether charges are the generators of the infinitesimal transformation on the

field. In fact, using (2.9) it can be directly checked that

$$[\mathcal{Q}_f, \psi(x)] = i\delta_f\psi(x), \quad (2.18)$$

If we denote the conserved charges of translation, rotation, scaling and special conformal transformation in (2.17) with $P_\mu, M_{\mu\nu}, D, K_\mu$ respectively, it can be verified that they have an algebra given by

$$\begin{aligned} [M^{\mu\nu}, P^\lambda] &= i(\eta^{\mu\lambda}P^\nu - \eta^{\nu\lambda}P^\mu) \\ [M^{\mu\nu}, M^{\rho\sigma}] &= i(\eta^{\mu\rho}M^{\nu\sigma} - \eta^{\mu\sigma}M^{\nu\rho} - \eta^{\nu\rho}M^{\mu\sigma} + \eta^{\nu\sigma}M^{\mu\rho}) \\ [M^{\mu\nu}, K^\lambda] &= i(\eta^{\mu\lambda}K^\nu - \eta^{\nu\lambda}K^\mu) \\ [D, P^\mu] &= -iP^\mu, \quad [D, K^\mu] = iK^\mu \\ [K^\mu, P^\nu] &= i(2D\eta^{\mu\nu} + M^{\mu\nu}), \end{aligned} \quad (2.19)$$

with all other commutators being zero. The above algebra is known as the conformal algebra. Consequently, the transformations generate the conformal group. Note that the first two relations tell us the Poincaré group is a subgroup of the conformal group.

2.2 Emergent Relativistic Symmetry in Graphene

Graphene is a $2d$ single-layer allotrope of carbon. It is famous for its unusual electronic properties (see reviews [14, 27]). In particular, graphene can be used as a condensed matter system to simulate various QFT phenomena like anomalies [15, 28, 33], as well as models of holographic systems [34]. In this section, we will discuss the emergence of relativistic symmetry in graphene [12].

Let's start with the lattice description of graphene. The bonds that connect the nearest C carbon atoms can be described by sp^2 hybridization. Since the number of valence electrons in carbon is four and three of them is connected to three other carbon atoms, there is one free electron per carbon atom living in the p_z orbital. As a result, graphene has a hexagonal honeycomb lattice as shown in the figure.

The lattice is comprised of two inequivalent sublattices A and B. Let's take two basis vectors

$$\vec{a}_1 = \frac{1}{2}(3, \sqrt{3})a, \quad \vec{a}_2 = \frac{1}{2}(3, -\sqrt{3})a \quad (2.20)$$

2.2. Emergent Relativistic Symmetry in Graphene

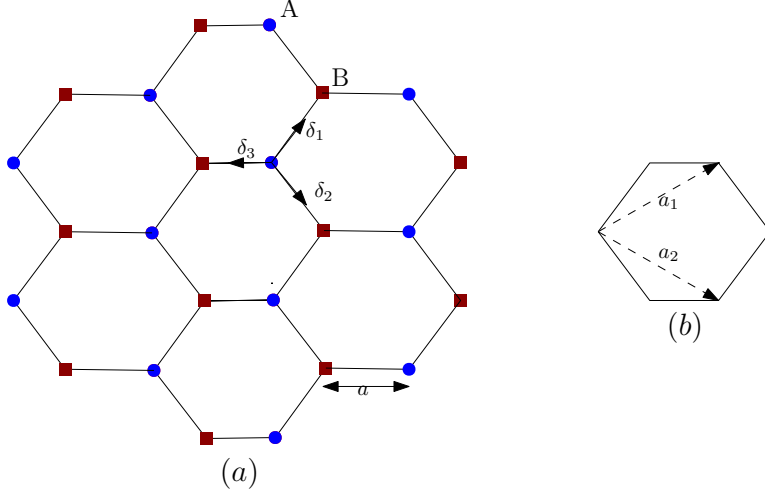


Figure 2.1: a) The hexagonal lattice structure of graphene is comprised of two inequivalent sublattice atoms, denoted here by A and B. b) A choice of basis vector for the A sublattice. Acting on by $m\vec{a}_1 + n\vec{a}_2$ with m, n integers, it is possible to move around between all A points.

where $a = 1.42\text{\AA}$ is the lattice constant. Each A atom is connected to three B atoms via vectors

$$\vec{\delta}_1 = \frac{1}{2}(1, \sqrt{3})a, \quad \vec{\delta}_2 = \frac{1}{2}(1, -\sqrt{3})a, \quad \vec{\delta}_3 = (-1, 0)a. \quad (2.21)$$

The simplest Hamiltonian for the system is described by the tight-binding model. To the first approximation, we only consider each electron can only hop to the nearest neighbor atom. This gives the following Hamiltonian for graphene in terms of fermionic annihilation and creation operators in sites A and B as

$$H = \sum_{i=1}^3 \sum_{\mathbf{n}, \sigma} [t a_{\mathbf{n}, \sigma}^\dagger b_{\mathbf{n}, \sigma + \delta_i} + h.c.]; \quad (2.22)$$

where $|t| \approx 2.8eV$ is the hopping parameter, $\sigma = \{\uparrow, \downarrow\}$ stands for the spin, and $h.c.$ denotes hermitian conjugation. To further analyze the system, next we write the operators $a_{n, \sigma}, b_{n, \sigma}$ in terms of Bloch waves

2.2. Emergent Relativistic Symmetry in Graphene

by defining a column vector

$$\psi_{\mathbf{n},\sigma} \equiv \begin{bmatrix} a_{\mathbf{n},\sigma} \\ b_{\mathbf{n},\sigma} \end{bmatrix} = \frac{1}{\sqrt{N}} \sum_{j=1}^3 \sum_{\vec{k}} \begin{bmatrix} \alpha_{\vec{k},\sigma} e^{i\vec{k}\cdot\vec{R}_{\mathbf{n}}} \\ \beta_{\vec{k},\sigma} e^{i\vec{k}\cdot(\vec{R}_{\mathbf{n}}+\delta_j)} \end{bmatrix}, \quad (2.23)$$

where $\vec{R}_{\mathbf{n}} = n_1\vec{a}_1 + n_2\vec{a}_2$ is the position of an arbitrary lattice site A spanned by the unit vectors and N is the number of unit cells. The Hamiltonian takes the form

$$H = \sum_{\vec{k}} \begin{bmatrix} a_{\vec{k},\sigma}^\dagger & b_{\vec{k},\sigma}^\dagger \end{bmatrix} \begin{bmatrix} 0 & \Delta(\vec{k}) \\ \Delta^*(\vec{k}) & 0 \end{bmatrix} \begin{bmatrix} a_{\vec{k},\sigma} \\ b_{\vec{k},\sigma} \end{bmatrix} \quad (2.24)$$

here

$$\Delta(\vec{k}) = t \sum_{j=1}^3 e^{i\vec{k}\cdot\vec{\delta}_j} \quad (2.25)$$

The energy eigenvalues

$$E_{\vec{k}} = \pm |\Delta(\vec{k})| \quad (2.26)$$

represent two energy bands respectively. So far our analysis have been exact. Now we shall concentrate on the low energy physics of the system. The zero of the energy can be found by solving the following equation

$$\begin{aligned} E_{\vec{k}} &= 0 \\ \text{or, } e^{i\vec{k}\cdot\vec{\delta}_1} + e^{i\vec{k}\cdot\vec{\delta}_2} + e^{i\vec{k}\cdot\vec{\delta}_3} &= 0. \end{aligned}$$

After some rearrangement,

$$1 + e^{-i\sqrt{3}k_y a} + e^{-i\frac{3}{2}k_x a - i\frac{\sqrt{3}}{2}k_y a} = 0 \quad (2.27)$$

The above equation has the following six solutions

$$(k_x, k_y) = \frac{2\pi}{3a} \left(\pm 1, \pm \frac{1}{\sqrt{3}} \right), \frac{2\pi}{3a} \left(0, \pm \frac{2}{\sqrt{3}} \right) \quad (2.28)$$

These six points where the top and bottom bands touch each other i.e the energy is zero are called Dirac points. In fact, not all six points are

2.2. Emergent Relativistic Symmetry in Graphene

independent. Only two of them are independent. Let's take them to be

$$(K) = \frac{2\pi}{3a} \left(1, \frac{1}{\sqrt{3}} \right), \quad (K') = \frac{2\pi}{3a} \left(1, -\frac{1}{\sqrt{3}} \right). \quad (2.29)$$

Indeed, if we define two reciprocal lattice vectors¹

$$\vec{b}_1 = \frac{2\pi}{3a} \left(1, \sqrt{3} \right), \quad \vec{b}_2 = \frac{2\pi}{3a} \left(1, -\sqrt{3} \right), \quad (2.30)$$

then acting on the independent points (K) and (K') by these vectors takes us to the remaining Dirac points.

We will be interested in the low energy excitation of the system. Near the (K) and (K') points, we have, in the linear order in \vec{k}

$$\begin{aligned} \Delta^{(K)}(\vec{k}) &= -ie^{\frac{2\pi i}{3}} v_F (k_x + iK_y) \\ \Delta^{(K')}(\vec{k}) &= -ie^{\frac{2\pi i}{3}} v_F (k_x - iK_y), \end{aligned}$$

where $v_F = \frac{3at}{2}$. Ignoring the overall phase factor $-ie^{\frac{2\pi i}{3}}$, the Hamiltonian near these points takes the form

$$\begin{aligned} H^{(K)} &= v_F \begin{bmatrix} 0 & k_x - ik_y \\ k_x + ik_y & 0 \end{bmatrix} \\ H^{(K')} &= v_F \begin{bmatrix} 0 & k_x + ik_y \\ k_x - ik_y & 0 \end{bmatrix}. \end{aligned} \quad (2.31)$$

These two points (K) and (K') are called *valleys*. As it can be seen from the above expressions, the Hamiltonian is different in two valleys. However, for practical purpose it is very convenient to use same Hamiltonian but assign the valley index to the two component spinor instead. The spinors in two valleys are defined as

$$\psi_\sigma^{(K)}(\vec{k}) \equiv \begin{bmatrix} a_\sigma(\vec{k}) \\ b_\sigma(\vec{k}) \end{bmatrix}, \quad \psi_\sigma^{(K')}(\vec{k}) \equiv \begin{bmatrix} b_\sigma(\vec{k}) \\ a_\sigma(\vec{k}) \end{bmatrix}. \quad (2.32)$$

Even though we are calling the above column vectors spinors, they have nothing to do with the real spin of the electrons. In fact, the

¹These are defined from the real space unit vectors \vec{a}_i by $\vec{a}_i \cdot \vec{b}_j = 2\pi\delta_{ij}$

2.3. Ferromagnetic Edge State in Graphene

components of the spinor label the wave functions in A and B valleys. Replacing the sum over momenta with integral we rewrite (2.23) as

$$H = v_F \sum_{A,\sigma} \int_B d\vec{k} \psi_\sigma^{\dagger(A)}(\vec{k}) \begin{bmatrix} 0 & k_x - ik_y \\ k_x + ik_y & 0 \end{bmatrix} \psi_\sigma^{(A)}(\vec{k}) \quad (2.33)$$

where we integrate over the modes that are in the first Brillouin zone. Taking the inverse fourier transform we can write the above equation in position space as

$$H = v_F \sum_{A,\sigma} \int d^2x \psi_\sigma^{\dagger(A)}(x) \begin{bmatrix} 0 & \partial_x + i\partial_y \\ \partial_x - i\partial_y & 0 \end{bmatrix} \psi_\sigma^{(A)}(x). \quad (2.34)$$

From the Hamiltonian density above, it is easy to write down the equation of motion for the spinor $\psi_\sigma^{(A)}(x)$ in the Hisenberg picture²

$$i \frac{\partial}{\partial t} \psi_\sigma^{(A)}(x) = v_F \begin{bmatrix} 0 & \partial_x + i\partial_y \\ \partial_x - i\partial_y & 0 \end{bmatrix} \psi_\sigma^{(A)}(x). \quad (2.35)$$

Now let's define $(v_F t, x, y) = (x^0, x^1, x^2)$ and choose a representation of gamma matrices in $(2 + 1)$ dimension as $\gamma^0 = i\sigma_z, \gamma^1 = \sigma_y, \gamma^2 = \sigma_x$ where $(\sigma_x, \sigma_y, \sigma_z)$ are the Pauli matrices. With these the above equation becomes

$$\not{\partial} \psi_\sigma^{(A)}(x) = 0. \quad (2.36)$$

This is nothing but the relativistic massless Dirac equation.

2.3 Ferromagnetic Edge State in Graphene

Now we would like to consider a semi-inifinite graphene sheet. There are two principal ways of cutting the graphene. The resulting edge configurations are known as zigzag or armchair edges (figure 2.2)

²We have set $\hbar = 1$

2.3. Ferromagnetic Edge State in Graphene

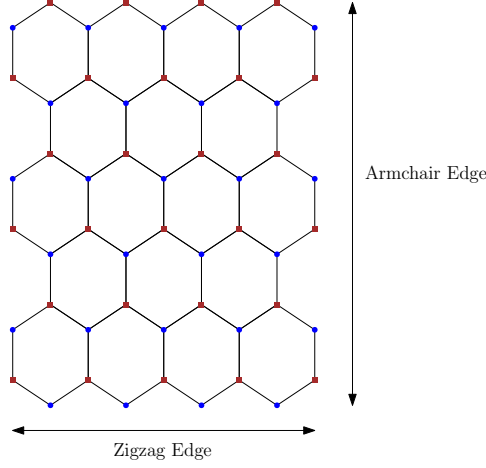


Figure 2.2: Two inequivalent ways of cutting the graphene sheet

The zigzag edge is composed of just one type of atom. Mathematically, this means one of the two components of the spinor is zero at the edge. The zigzag edge allows for zero-energy edge states called zero modes. Fermion zero modes give rise to a plethora of remarkable phenomena in condensed matter physics like fractional charge [18, 29], topological order [32] and various anomalies. In the context of graphene nano-ribbons, these edge-zero modes have been predicted to show magnetic order when electron-electron interaction is taken into account [13, 20]. In this section, we shall provide a much simpler argument for edge ferromagnetism in *semi-infinite* zigzag edge based on symmetries.

We model our system to be defined in the half-plane $x \geq 0$ with the boundary at $x = 0$. The low energy Dirac equation graphene can be derived from the action

$$\begin{aligned} \mathcal{S} &= \int_{-\infty}^{\infty} dt \int_{-\infty}^{\infty} dx \int_0^{\infty} dy \mathcal{L}(x) \\ \mathcal{L}(x) &= -\frac{i}{2} \left[\sum_{A,\sigma} \bar{\Psi}_{\sigma}^A(x) \left(\overleftarrow{\partial} - \overrightarrow{\partial} \right) \Psi_{\sigma}^A(x) \right] \end{aligned} \quad (2.37)$$

using the variational principle. The zigzag boundary condition can be modeled by

$$(1 + i\gamma^0)\Psi_{\sigma}^{(K)}(t, 0, y) = 0 = (1 - i\gamma^0)\Psi_{\sigma}^{(K')}(t, 0, y), \quad (2.38)$$

2.3. Ferromagnetic Edge State in Graphene

for (K) and (K') valleys respectively. In terms of the spinor components, the boundary condition (2.38) simply means one of the two components of the spinor vanishes at the boundary. It is easy to check that the variational problem is well-defined with the boundary condition (2.38).

Due to the presence of a planar boundary at $x = 0$, not all conformal transformations in (2.17) are allowed. The symmetries that remain are those for which the component of $f^\mu(x)$ vanishes as $x \rightarrow 0$. These are essentially the transformations that leave the boundary intact. This implies we must have $a^1 = 0, \omega^{0\mu} = 0$ and $b^1 = 0$. Thus for a planar boundary, the full conformal group $SO(3, 2)$ is 2 + 1 dimensions is reduced to $SO(2, 2)$.³ The spinor field transforms as

$$\delta_f \Psi_\sigma^{(A)}(x) = \left[f^\mu(x) \partial_\mu + \frac{1}{4} \epsilon^{\mu\nu\lambda} \gamma_\lambda \partial_\mu f_\nu(x) + \frac{1}{3} \partial_\mu f^\mu(x) \right] \Psi_\sigma^{(A)}(x). \quad (2.39)$$

However, the transformed field must also satisfy the boundary condition (2.38). Since, the boundary condition does not commute with $\gamma^{1,2}$ we see that the only consistent transformations are

$$\begin{aligned} \delta_H \Psi_\sigma^{(A)}(x) &= i \partial_t \Psi_\sigma^{(A)}(x), && \text{(Hamiltonian)} \\ \delta_P \Psi_\sigma^{(A)}(x) &= i \partial_y \Psi_\sigma^{(A)}(x), && \text{(Momentum along boundary)} \\ \delta_\Delta \Psi_\sigma^{(A)}(x) &= i (x \partial_x + y \partial_y + t \partial_t + 1) \Psi_\sigma^{(A)}(x), && \text{(Dilatation)}. \end{aligned} \quad (2.40)$$

Thus this system breaks both Lorentz and full conformal symmetry and there is no closed algebra between the conserved charges. Rather they satisfy

$$[H, P] = 0 \quad (2.41)$$

$$[\Delta, P] = P \quad (2.42)$$

$$[\Delta, H] = H \quad (2.43)$$

Finally, the phase transformation $\delta_N \Psi_\sigma^{(A)}(x) = e^{i\theta} \Psi_\sigma^{(A)}(x)$ is also compatible with the boundary condition. The corresponding conserved

³In fact, this is general result of CFT – a planar boundary reduces the full conformal group $SO(d, 2)$ to $SO(d - 1, 2)$.

2.3. Ferromagnetic Edge State in Graphene

charge is defined as⁴

$$N = \frac{1}{2} \sum_{A,\sigma} \int d^2x [\psi_\sigma^{(A)\dagger}, \psi_\sigma^{(A)}]. \quad (2.44)$$

Together with the three operators mentioned above, the set $\{N, H, P, \Delta\}$ constitutes the conserved charges of the system under continuous symmetry transformations.

The second quantized wave function can be found by solving the Dirac equation with appropriate boundary conditions. Explicitly we have,

$$\begin{aligned} \Psi_\sigma^{(K)}(x, y, t) &= \\ &= \int_{-\infty}^{\infty} dk \int_0^{\infty} \frac{d\ell}{\sqrt{2\pi}} \left[\begin{array}{c} i \frac{k \sin \ell x + \ell \cos \ell x}{\sqrt{k^2 + \ell^2}} \\ \sin \ell x \end{array} \right] e^{iky - i\omega t} a_\sigma^{(K)}(k, \ell) \\ &+ \int_{-\infty}^{\infty} dk \int_0^{\infty} \frac{d\ell}{\sqrt{2\pi}} \left[\begin{array}{c} i \frac{k \sin \ell x - \ell \cos \ell x}{\sqrt{k^2 + \ell^2}} \\ \sin \ell x \end{array} \right] e^{-iky + i\omega t} b_\sigma^{(K)\dagger}(k, \ell) \\ &+ \left[\begin{array}{c} 1 \\ 0 \end{array} \right] \int_{-\infty}^0 \frac{|k|^{\frac{1}{2}} dk}{\sqrt{\pi}} e^{k(x+iy)} \alpha_\sigma^{(K)}(k) \end{aligned} \quad (2.45)$$

and for the other valley,

$$\begin{aligned} \Psi_\sigma^{(K')}(x, y, t) &= \\ &= \int_{-\infty}^{\infty} dk \int_0^{\infty} \frac{d\ell}{\sqrt{2\pi}} \left[\begin{array}{c} \sin \ell x \\ i \frac{-k \sin \ell x + \ell \cos \ell x}{\sqrt{k^2 + \ell^2}} \end{array} \right] e^{iky - i\omega t} a_\sigma^{(K')}(k, \ell) \\ &+ \int_{-\infty}^{\infty} dk \int_0^{\infty} \frac{d\ell}{\sqrt{2\pi}} \left[\begin{array}{c} \sin \ell x \\ i \frac{-k \sin \ell x - \ell \cos \ell x}{\sqrt{k^2 + \ell^2}} \end{array} \right] e^{-iky + i\omega t} b_\sigma^{(K')\dagger}(k, \ell) \\ &+ \left[\begin{array}{c} 0 \\ 1 \end{array} \right] \int_0^{\infty} \frac{|k|^{\frac{1}{2}} dk}{\sqrt{\pi}} e^{-k(x-iy)} \alpha_\sigma^{(K')}(k) \end{aligned} \quad (2.46)$$

where $\omega = v_F \sqrt{k^2 + l^2}$. We have introduced the electron, hole and zero-mode creation and annihilation operators having non-vanishing

⁴This definition is chosen so the the number operators respects particle-hole symmetry $N \longleftrightarrow -N$ when $\psi_\sigma^{(A)\dagger} \longleftrightarrow \psi_\sigma^{(A)}$

2.3. Ferromagnetic Edge State in Graphene

anti-commutation relations

$$\begin{aligned}
\left\{ a_{\sigma}^{(A)}(k, \ell), a_{\sigma'}^{(A')\dagger}(k', \ell') \right\} &= \delta^{AA'} \delta_{\sigma\sigma'} \delta(k - k') \delta(\ell - \ell') \\
\left\{ b_{\sigma}^{(A)}(k, \ell), b_{\sigma'}^{(A')\dagger}(k', \ell') \right\} &= \delta^{AA'} \delta_{\sigma\sigma'} \delta(k - k') \delta(\ell - \ell'). \quad (2.47) \\
\left\{ \alpha_{\sigma}^{(A)}(k), \alpha_{\sigma'}^{(A')\dagger}(k') \right\} &= \delta^{AA'} \delta_{\sigma\sigma'} \delta(k - k')
\end{aligned}$$

The states of this system are gotten from a vacuum state which is annihilated by the annihilation operators for all of the bulk modes.

$$a_{\sigma}^{(A)}(k, \ell) |0\rangle, \quad b_{\sigma}^{(A)}(k, \ell) |0\rangle, \quad \forall k, l, A, \sigma, \quad \langle 0|0\rangle. \quad (2.48)$$

Then, we must decide on how the zero mode operators $\alpha_{\sigma}^{(A)}(k), \alpha_{\sigma}^{(A)\dagger}(k)$ act on this state. Since they annihilate and create excitations with zero energy, all of the possibilities are degenerate, any filling of the zero modes has the same energy as any other filling.

Since our ground state should be invariant under the residual symmetries first let us express the charges in terms of the oscillators. They take the form

$$\begin{aligned}
H &= [\dots] \\
P &= \sum_{\sigma} \left[\int_{-\infty}^0 dk k \alpha_{\sigma}^{\dagger(K)}(k) \alpha_{\sigma}^{(K)}(k) + \int_0^{\infty} dk k \alpha_{\sigma}^{\dagger(K')}(k) \alpha_{\sigma}^{(K')}(k) \right] + [\dots] \\
\Delta &= \sum_{\sigma} \left[\int_{-\infty}^0 dk \alpha_{\sigma}^{\dagger(K)}(k) \left(k \frac{d}{dk} + \frac{1}{2} \right) \alpha_{\sigma}^{(K)}(k) \right. \\
&\quad \left. + \int_0^{\infty} dk \alpha_{\sigma}^{\dagger(K')}(k) \left(k \frac{d}{dk} + \frac{1}{2} \right) \alpha_{\sigma}^{(K')}(k) \right] + [\dots] \\
N &= \frac{1}{2} \sum_{\sigma} \left(\int_{-\infty}^0 dk [\alpha_{\sigma}^{\dagger(K)}(k), \alpha_{\sigma}^{(K)}(k)] + \int_0^{\infty} dk [\alpha_{\sigma}^{\dagger(K')}(k), \alpha_{\sigma}^{(K')}(k)] \right. \\
&\quad \left. + [\dots] \right) \quad (2.49)
\end{aligned}$$

Here we have written out explicitly the portion that depends on the zero modes and the [...] stands for non-zero modes. The Hamiltonian H does not depend on the zero-modes as expected. First, we note that the ordering of the creation and annihilation operator is ambiguous

2.3. Ferromagnetic Edge State in Graphene

because of the absence of any algebra. Using this freedom, we define two states that are annihilated by P, Δ as

Definition 2. *The state that is annihilated by all annihilation operators $\alpha_\sigma^{(A)}(k) |\mathcal{E}\rangle_\sigma^{(A)} = 0$; $\forall k, \sigma, A$ is called a **completely empty state**.*

*The state that is annihilated by all creation operators $\alpha_\sigma^{\dagger(A)}(k) |\mathcal{F}\rangle_\sigma^{(A)} = 0$; $\forall k, \sigma, A$ is called a **completely full state**.*

However, both states are highly charged as can be seen by acting on the number operator:

$$\begin{aligned} N |\mathcal{E}\rangle_\sigma^{(A)} &= -\infty \\ N |\mathcal{F}\rangle_\sigma^{(A)} &= +\infty. \end{aligned} \quad (2.50)$$

In fact, to be annihilated by N , the states have to be half-filled. But, those states will not be annihilated by P and D . We discover an *anomaly* implying for *one* species of electron, there is no such state that is annihilated by all for operators $\{H, P, \Delta, N\}$.

Let us try to solve this issue by including multiple species with valley indices K, K' respectively and constructing a state that respects the discrete symmetries of the system. We define the action of parity (\mathcal{P}), charge conjugation (\mathcal{C}) and \mathcal{CP} as follows:

$$\begin{aligned} \mathcal{P} : \quad \Psi_\sigma^{(K)}(x, y, t) &\longrightarrow \gamma^2 \Psi_\sigma^{(K')}(x, -y, t); & \alpha_\sigma^{(K)}(k) &\rightarrow \alpha_\sigma^{K'}(-k) \\ \mathcal{C} : \quad \Psi_\sigma^{(K)}(x, y, t) &\longrightarrow \gamma^2 \Psi_\sigma^{*(K')}(x, y, t); & \alpha_\sigma^{(K)}(k) &\rightarrow \alpha_\sigma^{\dagger(K')}(-k) \\ \mathcal{CP} : \quad \Psi_\sigma^{(K)}(x, y, t) &\longrightarrow \Psi_\sigma^{*(K)}(x, -y, t); & \alpha_\sigma^{(K)}(k) &\rightarrow \alpha_\sigma^{\dagger(K)}(k) \end{aligned}$$

Using the above transformation rules, we see the empty and full states in each valley transform as:

$$\mathcal{P} : \quad |\mathcal{E}\rangle_\sigma^{(K)} \longleftrightarrow |\mathcal{E}\rangle_\sigma^{(K')}; \quad |\mathcal{F}\rangle_\sigma^{(K)} \longleftrightarrow |\mathcal{F}\rangle_\sigma^{(K')}, \quad (2.51)$$

$$\mathcal{C} : \quad |\mathcal{E}\rangle_\sigma^{(K)} \longleftrightarrow |\mathcal{F}\rangle_\sigma^{(K')}; \quad |\mathcal{F}\rangle_\sigma^{(K)} \longleftrightarrow |\mathcal{E}\rangle_\sigma^{(K')}, \quad (2.52)$$

$$\mathcal{CP} : \quad |\mathcal{E}\rangle_\sigma^{(K)} \longleftrightarrow |\mathcal{F}\rangle_\sigma^{(K)}; \quad |\mathcal{F}\rangle_\sigma^{(K)} \longleftrightarrow |\mathcal{E}\rangle_\sigma^{(K)}. \quad (2.53)$$

From the above relations, a careful thought reveals that there is no state that is allowed by above symmetries if we keep the spin degree of freedom untouched.

2.3. Ferromagnetic Edge State in Graphene

To resolve this issue, we shall use the spin degeneracy in graphene. To this end, let us define a \mathcal{CP} symmetry along with spin flip namely,

$$\mathcal{CP} + \mathcal{S} : \quad \Psi_{\sigma}^{(K)}(x, y, t) \longrightarrow \Psi_{-\sigma}^{*(K)}(x, -y, t); \quad \alpha_{\sigma}^{(K)}(k) \rightarrow \alpha_{-\sigma}^{\dagger(K)}(k), \quad (2.54)$$

Such a symmetry is consistent with the boundary conditions (2.38). Under this symmetry we have

$$\mathcal{CP} + \mathcal{S} : \quad |\mathcal{E}\rangle_{\sigma}^{(K)} \longleftrightarrow |\mathcal{F}\rangle_{-\sigma}^{(K)}; \quad |\mathcal{E}\rangle_{\sigma}^{(K')} \longleftrightarrow |\mathcal{F}\rangle_{-\sigma}^{(K')}. \quad (2.55)$$

There are two ways to achieve this. For instance, we can augment the charge conjugation symmetry to include spin flip and leave the parity symmetry untouched. $\mathcal{C} + \mathcal{S}$ implies

$$\mathcal{C} + \mathcal{S} : \quad |\mathcal{E}\rangle_{\sigma}^{(K)} \longleftrightarrow |\mathcal{F}\rangle_{-\sigma}^{(K')}, \quad |\mathcal{F}\rangle_{\sigma}^{(K)} \longleftrightarrow |\mathcal{E}\rangle_{-\sigma}^{(K')}. \quad (2.56)$$

The state consistent with this symmetries is

$$|\mathcal{O}\rangle_1 = |\mathcal{E}\rangle_{\sigma}^{(K)} |\mathcal{F}\rangle_{-\sigma}^{(K)} |\mathcal{E}\rangle_{\sigma}^{(K')} |\mathcal{F}\rangle_{-\sigma}^{(K')}. \quad (2.57)$$

This state is ferromagnetic.

Alternatively, we could also augment the parity to include spin flip leaving charge conjugation. $\mathcal{P} + \mathcal{S}$ implies

$$\mathcal{P} + \mathcal{S} : \quad |\mathcal{E}\rangle_{\sigma}^{(K)} \longleftrightarrow |\mathcal{E}\rangle_{-\sigma}^{(K')}, \quad |\mathcal{E}\rangle_{\sigma}^{(K')} \longleftrightarrow |\mathcal{F}\rangle_{-\sigma}^{(K')}. \quad (2.58)$$

The corresponding state takes the form

$$|\mathcal{O}\rangle_2 = |\mathcal{E}\rangle_{\sigma}^{(K)} |\mathcal{F}\rangle_{-\sigma}^{(K)} |\mathcal{E}\rangle_{-\sigma}^{(K')} |\mathcal{F}\rangle_{\sigma}^{(K')}. \quad (2.59)$$

This state is anti-ferromagnetic.

To resolve the degeneracy, let's turn on a small constant magnetic field. The magnetic field breaks both \mathcal{C} and \mathcal{P} since under those it transforms as $B \rightarrow -B$ [35]. Additionally, it also breaks the scaling symmetry. However, it preserves \mathcal{CP} , since it maps $B \rightarrow B$. The effect of turning on a magnetic field on zero modes is rather dramatic. For small constant $B > 0$, the eigenvalue equation for zero-mode takes the following form in the symmetric gauge $\vec{A} = -\frac{B}{2}(y, -x)$ as

$$\left[\begin{array}{cc} 0 & \partial_x + i\partial_y + \frac{B}{2}(x + iy) \\ \partial_x - i\partial_y - \frac{B}{2}(x + iy) & 0 \end{array} \right] \psi_{\sigma}^{(A)}(x) = 0 \quad (2.60)$$

2.3. Ferromagnetic Edge State in Graphene

Imposing the boundary condition (2.38) and keeping on the solutions that are regular at infinity we obtain

$$\psi_{\sigma}^{(K)} = \begin{bmatrix} e^{-\frac{B}{4}(x^2+y^2)} f(x+iy) \\ 0 \end{bmatrix}, \quad \psi_{\sigma}^{(K')} = \begin{bmatrix} 0 \\ 0 \end{bmatrix}, \quad B > 0 \quad (2.61)$$

where $f(x+iy)$ is an appropriately normalized arbitrary function. That is all modes populate one valley and the other valley is completely empty. Since the graphene as a whole is electrically neutral, the ground state must be half-filled with the zero-mode excitations. Additionally, since all the electrons sit in the same lattice and they have the same valley index they must take the same spin index so that the Coulomb repulsion is minimum. This situation is similar to Hund's rule. Thus the resulting state is ferromagnetic.

When B is reduced to zero, scale invariance is restored and both valleys are populated with zero modes and the resulting state should be ferromagnetic as in (2.57). Finally, when $B < 0$, all zero-mode excitations move to the other valley.

Thus we see that the ferromagnetic state (2.57) is consistent with a smooth variation of magnetic field and should be the preferred state in a semi-infinite graphene sheet. We conclude this section with a few comments. First, if we had only one species of electron, parity and charge conjugation would be broken for the system. However, the combined \mathcal{CP} symmetry would be preserved so there will be no observable effect of braking of the individual symmetries. In this sense, this system is immune to many symmetry-breaking phenomena. Finally, to our knowledge, the dramatic behavior of zero-mode depending on the sign of the magnetic field has not been reported in the literature yet and requires more investigation.

Chapter 3

Conformal Field theory

This chapter serves as a general introduction to the conformal and boundary conformal field theory. For more details on the subject, we refer the reader to [3, 6, 11, 25].

3.1 Conformal transformations in d dimensions

The starting point of Conformal field theory is to understand the conformal transformation (CT). Conformal transformations are the special kind of coordinate transformations that preserve the angle. Hence, they keep the “shape” unchanged, but the “size” can change. As a result of CTs, the metric changes by an overall factor, say $\Lambda^2(x)$.

Formally, we know that the metric $g_{\mu\nu}(x)$, being a tensor of rank two, changes as $g'_{\mu\nu}(x') = \frac{\partial x^\rho}{\partial x'^\mu} \frac{\partial x^\sigma}{\partial x'^\nu} g_{\rho\sigma}(x)$ under *any* coordinate transformation $x \rightarrow x'$. A *conformal transformation* is defined in the following way:

Definition 3. A transformation $x^\mu \rightarrow x'^\mu$ is called a conformal transformation, if it changes the metric as

$$g_{\mu\nu}(x) \rightarrow g'_{\mu\nu}(x') = \Lambda^2(x)g_{\mu\nu}(x) \quad (3.1)$$

Note that if $\Lambda(x) = 1$, the metric remains unaffected and we recover the Poincare group consisting translations and Lorentz transformations. Thus, Poincare group is a subgroup of the conformal group as expected.

Let us work in the flat background $g_{\mu\nu} = \eta_{\mu\nu}$. Next, we consider infinitesimal transformations $x'^\mu = x^\mu + f^\mu(x)$. Substituting in (3.1) and taking trace on both sides we obtain $\Lambda^2(x) = 1 + \frac{2}{d}\partial \cdot f$. This in turns gives

$$\partial^\mu f^\nu + \partial^\nu f^\mu = \frac{2}{d}\partial \cdot f. \quad (3.2)$$

3.2. CFT in $d = 2$ dimensions

This equation is called the **conformal killing equation** and the $f^\mu(x)$ that satisfy (3.2) are called **conformal killing vectors**.

The conformal killing equation (3.2) has the following solutions

$$\begin{aligned}
 f^\mu &= a^\mu && \text{(Translation)} \\
 f^\mu &= \omega^{\mu\nu} x_\nu && \text{(Rotation)} \\
 f^\mu &= \lambda x^\mu && \text{(Scaling)} \\
 f^\mu &= x^\mu (b \cdot x) - \frac{1}{2} b^\mu x^2 && \text{(Special conformal transformation),}
 \end{aligned}$$

where λ, a^μ, b^μ are constants and $\omega^{\mu\nu} = -\omega^{\nu\mu}$. It's easy to count how many conformal killing vectors we have. In d dimensions, we have one scaling transformation, d translations, d special conformal transformations and $\frac{1}{2}d(d-1)$ rotations. In total we have $\frac{1}{2}(d+1)(d+2)$ conformal killing vectors. The conformal group is isomorphic to the $SO(d, 2)$ group which has the same number of generators.

3.2 CFT in $d = 2$ dimensions

The mathematical structure of conformal transformations is very rich in two dimensions. Putting $d = 2$ in our conformal Killing equation (3.2) we obtain

$$\partial_0 f_0 = \partial_1 f_1, \quad \partial_0 f_1 = -\partial_1 f_0. \quad (3.3)$$

Let us go to complex coordinates by defining

$$\begin{aligned}
 z &= x^0 + ix^1, & \bar{z} &= x^0 - ix^1. \\
 f &= f_0 + if_1, & \bar{f} &= f_0 - if_1 \\
 \partial_0 &= \partial_z + \partial_{\bar{z}}, & \partial_1 &= i(\partial_z - \partial_{\bar{z}}).
 \end{aligned} \quad (3.4)$$

Using this we obtain from (3.3)

$$\partial_z \bar{f} = 0, \quad \partial_{\bar{z}} f = 0. \quad (3.5)$$

This implies any holomorphic $f \equiv f(z)$ and anti-holomorphic $\bar{f} \equiv \bar{f}(\bar{z})$ is an acceptable conformal transformation in $d = 2$. Consequently,

3.2. CFT in $d = 2$ dimensions

there is an infinite number of them. Alternatively, the two dimensional Euclidean flat metric can be rewritten as

$$\begin{aligned} ds^2 &= (dx^0)^2 + (dx^1)^2 \\ &= dzd\bar{z}. \end{aligned} \tag{3.6}$$

Consider a infinitesimal transformation

$$z' = z + f(z), \quad \bar{z}' = \bar{z} + \bar{f}(\bar{z}). \tag{3.7}$$

We can rewrite the metric in primed coordinate in terms of the unprimed one as

$$\begin{aligned} ds'^2 &= dz'd\bar{z}' \\ &= \left| \frac{df}{dz} \right|^2 dzd\bar{z}. \end{aligned} \tag{3.8}$$

The fact that the number of allowed transformations is infinite is very different than $d \geq 3$ where we only had finite candidates. This gives the CFT in $d = 2$ a rich mathematical structure some of which we will explore in this section. It is very convenient and natural to work in the complex coordinate and treat z, \bar{z} as independent coordinates. Moreover, we will take our system to be defined in the Riemann sphere $S^2 = \mathbb{C} \cup \infty$.

Our goal is to construct a QFT that respects the conformal symmetry. We start by defining what we mean by field.

Definition 4. A field $\phi(z, \bar{z})$ is called a **primary field** of conformal dimension (h, \bar{h}) if it transforms under a conformal transformation $z \rightarrow f(z)$ as

$$\phi(z, \bar{z}) \rightarrow \left(\frac{\partial \tilde{f}}{\partial z} \right)^h \left(\frac{\partial \bar{\tilde{f}}}{\partial \bar{z}} \right)^{\bar{h}} \phi(f(z), \bar{f}(\bar{z})). \tag{3.9}$$

A field that is not a primary field is called a secondary field.

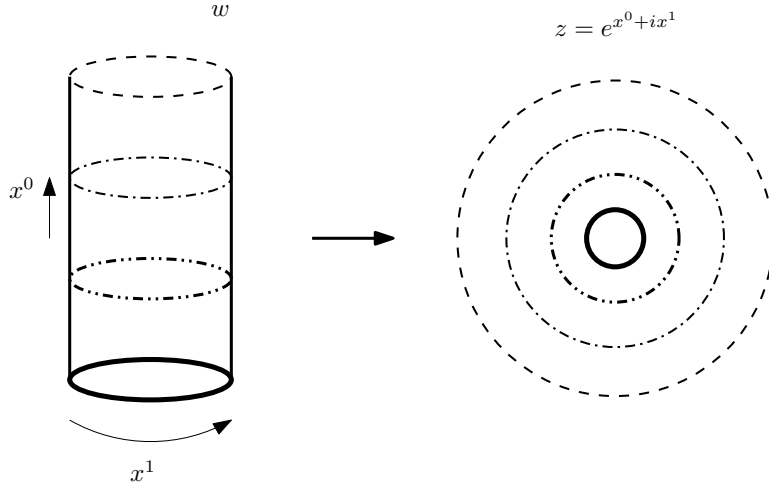


Figure 3.1: In the cylinder time runs along the length of the cylinder and the space direction is compactified in a circle. The cylinder is mapped to the complex plane by mapping $z = e^w$, $w = x^0 + ix^1$.

In QFT the process of quantization is usually done in constant time-slice. Fields that are representations of the symmetry group of the theory then obey *equal time* commutation or anti-commutation relations on this hyperspace. Since we are working in Euclidean signature, there is no natural notion of time for us. However, we can still make some connections with the Minkowski space by adopting a scheme called the **radial quantization**. We define a space direction by a circle $x \sim x + 2\pi$ and take the time direction t running perpendicular to the plane of the circle. This way we obtain a cylinder. With this definition, the time translation $t \rightarrow t + a$ becomes a dilatation $z \rightarrow e^a z$ and the spacial translations $x \rightarrow x + b$ corresponds to rotation $z \rightarrow e^{ib} z$ in the complex plane.

3.2.1 Virasoro Algebra

As mentioned in the previous section, there is an infinite number of conformal transformations in two dimensions. Consequently, there is an infinite number of conserved charges. In quantum theory, the algebra that the conserved charges obey is known as this algebra. In this section, we will derive the Virasoro algebra. Along the way, we will discuss a very important concept in CFT known as the operator prod-

3.2. CFT in $d = 2$ dimensions

uct expansion (OPE). To begin with, let us assume that there exists a quantity called the energy-momentum tensor defined as follows

Definition 5. *Given an action S of the theory one can define a symmetric tensor called the **energy-momentum tensor** as*

$$T_{\mu\nu}(x) = \frac{\delta S}{\delta g_{\mu\nu}(x)} \quad (3.10)$$

The symmetric property of $T_{\mu\nu}$ is apparent from the definition. Additionally, $T_{\mu\nu}$ satisfies

$$\partial_\mu T^{\mu\nu} = 0. \quad (3.11)$$

From the energy-momentum tensor we can define the conserved current

$$j^\mu = T^{\mu\nu} f_\nu, \quad (3.12)$$

where f_μ is a conformal killing vector. The current is conserved if $T_{\mu\nu}$ is traceless. Namely

$$\begin{aligned} \partial_\mu j^\mu &= T^{\mu\nu} \partial_\mu f_\nu \\ &= \frac{1}{2} T^{\mu\nu} (\partial_\mu f_\nu + \partial_\nu f_\mu) \\ &= \frac{1}{d} T^\mu{}_\mu. \end{aligned} \quad (3.13)$$

Thus if $T^\mu{}_\mu = 0$, j^μ is a conserved current.

In terms of the complex coordinates in $d = 2$ we have the following relations

$$\begin{aligned} T_{zz} &= \frac{1}{4}(T_{00} - 2iT_{01} - T_{11}), \\ T_{\bar{z}\bar{z}} &= \frac{1}{4}(T_{00} + 2iT_{01} - T_{11}), \\ T_{z\bar{z}} &= T_{\bar{z}z} = \frac{1}{4}(T_{00} + T_{11}) \end{aligned}$$

Using the tracelessness condition $T_{00} + T_{11} = 0$ we obtain

$$\begin{aligned} T_{zz} &= \frac{1}{2}(T_0 - iT_{01}), \\ T_{\bar{z}\bar{z}} &= \frac{1}{2}(T_0 + iT_{01}), \\ T_{z\bar{z}} &= T_{\bar{z}z} = 0. \end{aligned}$$

3.2. CFT in $d = 2$ dimensions

The conservation law (3.11) reads

$$\partial_{\bar{z}}T_{zz} = 0, \quad \partial_z T_{\bar{z}\bar{z}} = 0 \quad (3.14)$$

This implies $T_{zz} \equiv T(z)$ is a holomorphic function and $T_{\bar{z}\bar{z}} \equiv \bar{T}(\bar{z})$ is an anti-holomorphic function.

In QFT, one defines a conserved charge from the conserved current as

$$Q = \int dx j^0 \quad (3.15)$$

This charge generates the symmetry transformation of the field ϕ in the quantum theory

$$\delta\phi = [Q, \phi] \quad (3.16)$$

and one needs to use the equal time commutation relations. In $d = 2$ from our radial quantization picture the integral over the spatial coordinate and $x^0 = \text{constant}$ becomes a contour integral. In $d = 2$ we define

$$\begin{aligned} Q &= \frac{1}{2\pi} \int dx^1 j_0 \\ &= \frac{1}{2\pi} \int dx^1 (j_z + j_{\bar{z}}) \\ &= \frac{1}{2\pi i} \oint (dz j_z - d\bar{z} j_{\bar{z}}) \\ &= \frac{1}{2\pi i} \left(\oint_C dz f(z) T(z) - \oint_{\bar{C}} d\bar{z} \bar{f}(\bar{z}) \bar{T}(\bar{z}) \right) \end{aligned} \quad (3.17)$$

where in the last line, we assumed that the current factorizes into holomorphic and anti-holomorphic part. The integral contours are defined so that

$$\oint_C \frac{1}{2\pi i} \frac{1}{z} dz = 1, \quad -\frac{1}{2\pi i} \oint_{\bar{C}} \frac{1}{\bar{z}} d\bar{z} = 1.$$

Thus the variation of a field is given by

$$\delta\phi(w, \bar{w}) = \frac{1}{2\pi i} \left(\oint_C dz f(z) [T(z), \phi(w, \bar{w})] - \oint_{\bar{C}} d\bar{z} \bar{f}(\bar{z}) [\bar{T}(\bar{z}), \phi(w, \bar{w})] \right) \quad (3.18)$$

3.2. CFT in $d = 2$ dimensions

If ϕ is a primary field, the left hand side of the above equation is easy to determine from the definition of ϕ

$$\begin{aligned} \delta\phi(w, \bar{w}) &= \left(\frac{\partial \tilde{f}}{\partial w}\right)^h \left(\frac{\partial \bar{\tilde{f}}}{\partial \bar{w}}\right)^{\bar{h}} \phi(f(w), \bar{f}(\bar{w})) - \phi(w, \bar{w}) \\ &= (hf'(w) + f(w)\partial_w + \bar{h}\bar{f}'(\bar{w}) + \bar{f}(\bar{w})\partial_{\bar{w}})\phi(w, \bar{w}) \end{aligned} \quad (3.19)$$

where we have used $\tilde{f}(w) \sim w + f(w)$. However, the right-hand side only makes sense if w is inside of the contour z . In QFT, all correlation functions are usually time ordered. In radial quantization two times $t > w$ translates to two circles with radii $|z| > |w|$. Thus we define radial ordering of two operators as

$$R(A(z)B(w)) := \begin{cases} A(z)B(w) & \text{for } |z| > |w| \\ B(w)A(z) & \text{for } |w| > |z|. \end{cases} \quad (3.20)$$

This tells us how to interpret expressions like (see fig 3.2)

$$\oint dz (A(z)B(w) - B(w)A(z)) = \oint_{C(w)} dz R(A(z), B(w)) \quad (3.21)$$

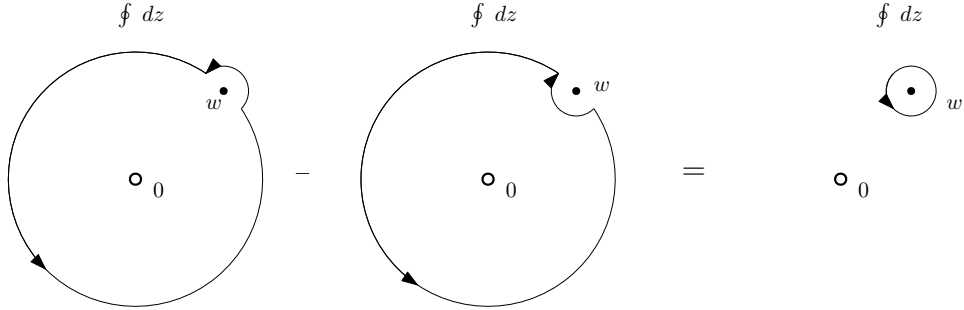


Figure 3.2: The integration contour of eq. (3.21) can be deformed into a contour tightly wound around w .

With this definition we can rewrite (3.18) as

$$\begin{aligned} &(hf'(w) + f(w)\partial_w)\phi(w, \bar{w}) + \text{anti-holomorphic} \\ &= \frac{1}{2\pi i} \oint_C dz R(T(z)\phi(w, \bar{w})) + \text{anti-holomorphic} \end{aligned} \quad (3.22)$$

3.2. CFT in $d = 2$ dimensions

Using the following relations

$$\begin{aligned} hf'(w)\phi(w, \bar{w}) &= \frac{1}{2\pi i} \oint_{C(w)} dz \frac{hf(w)}{(z-w)^2} \phi(w, \bar{w}) \\ f(w)\partial_w\phi(w, \bar{w}) &= \frac{1}{2\pi i} \oint_{C(w)} dz \frac{f(w)}{(z-w)} \partial_w\phi(w, \bar{w}), \end{aligned}$$

we finally obtain

$$\begin{aligned} &\left[R(T(z)\phi(w, \bar{w})) - \frac{h}{(z-w)^2} \phi(w, \bar{w}) + \frac{1}{(z-w)} \partial_w\phi(w, \bar{w}) + \dots \right] \\ &+ \left[R(\bar{T}(\bar{z})\phi(w, \bar{w})) - \frac{\bar{h}}{(z-w)^2} \phi(w, \bar{w}) + \frac{1}{(z-w)} \partial_w\phi(w, \bar{w}) + \dots \right] = 0 \end{aligned} \tag{3.23}$$

Since the holomorphic and anti-holomorphic degrees are independent of each other, each of the relations in the parentheses is individually zero. The above equations are known as operator product expansion (OPE) for the primary field of conformal dimension (h, \bar{h}) .

The OPE of $T(z)$ with itself reads

$$T(z)T(w) = \frac{c/2}{(z-w)^4} + \frac{2T(w)}{(z-w)^2} + \frac{\partial_w T(w)}{(z-w)} + \dots, \tag{3.24}$$

where ... denotes the regular part. We omit the proof of this relation here. The quantity c is called the **central charge**. It depends on the theory and in some sense characterizes the particular CFT we are talking about. For example, free boson has $c = 1$ and free fermion has $c = 1/2$. The above OPE also shows that $T(z)$ is not a primary field. Hence, it does not transform according to (3.9). Instead, its transformation as a result of a coordinate change $z \rightarrow w(z)$ is given by

$$\tilde{T}(w) = (w'(z))^{-2} \left[T(z) + \frac{c}{12} s(w, z) \right] \tag{3.25}$$

where $s(w, z) := \frac{w'''(z)}{w'(z)} - \frac{3}{2} \left(\frac{w''(z)}{w'(z)} \right)^2$ is called the Schwarzian derivative.

Now we are ready to derive the Virasoro algebra. First we insert the

3.2. CFT in $d = 2$ dimensions

following Laurent series expansions in the definition of charge (3.17)

$$\begin{aligned}
 f(z) &= \sum_n c_n z^{n+1}, & \bar{f}(\bar{z}) &= \sum_n \bar{c}_n \bar{z}^{n+1} \\
 L(z) &= \sum_n z^{-n-2} L_n, & L_n &= \frac{1}{2\pi i} \oint dz z^{n+1} T(z) \\
 \bar{L}(\bar{z}) &= \sum_n \bar{z}^{-n-2} \bar{L}_n, & \bar{L}_n &= -\frac{1}{2\pi i} \oint d\bar{z} \bar{z}^{n+1} \bar{T}(\bar{z})
 \end{aligned}$$

This gives

$$Q = \sum_n c_n L_n + \sum_n \bar{c}_n \bar{L}_n \quad (3.26)$$

Next compute the commutator between two modes

$$\begin{aligned}
 [L_m, L_n] &= \frac{1}{(2\pi i)^2} \oint_0 dw w^{m+1} \oint_w dz z^{m+1} [T(w), T(z)] \\
 &= \frac{1}{(2\pi i)^2} \oint_0 dw w^{m+1} \oint_w dz z^{m+1} R(T(z)T(w)) \\
 &= \frac{1}{(2\pi i)^2} \oint_0 dw w^{m+1} \oint_w dz z^{m+1} \\
 &\quad \times \left[\frac{c/2}{(z-w)^4} + \frac{2T(w)}{(z-w)^2} + \frac{\partial_w T(w)}{(z-w)} + \dots \right] \\
 &= (n-m)L_{m+n} + \frac{c}{12} m(m^2-1) \delta_{m+n,0} \quad (3.27)
 \end{aligned}$$

Similarly one can derive

$$[\bar{L}_m, \bar{L}_n] = (n-m)\bar{L}_{m+n} + \frac{\bar{c}}{12} m(m^2-1) \delta_{m+n,0} \quad (3.28)$$

$$[\bar{L}_m, L_n] = 0 \quad (3.29)$$

The above relations are known as the Virasoro algebra. In the level of the algebra (c, \bar{c}) is called the central extension. This is unique to CFTs in $d = 2$. In higher dimensions, such an extension of the algebra of the conserved charges does not exist.

3.2.2 The Hilbert Space

Our task is to construct a representation of the Virasoro algebra derived in the previous section. As in QFT, we start from the vacuum and build up the excited states from it. The vacuum should be invariant under all conformal symmetries. Vacuum state satisfies

$$L_n |0\rangle = 0, \quad n \geq -1. \quad (3.30)$$

This relation can be derived from the definition of L_n and demanding the regularity of $T(z)$ at $z = 0$. In the radial quantized picture, an asymptotic state is created by inserting a field $\phi(z, \bar{z})$ of conformal weight h at the origin

$$|h\rangle := \phi(0, 0) |0\rangle. \quad (3.31)$$

This state is *asymptotic* in the sense that the time $t = -\infty$ is mapped to the origin in the radial quantization. To find a representation of the algebra (3.27), we take L_0 to be diagonal and define the highest weight state with the following property

$$L_0 |h\rangle = h |h\rangle. \quad (3.32)$$

Since, $[L_0, L_m] = -mL_m$, $L_m, m > 0$ and $L_{-m}, m > 0$ are lowering and raising operators for the highest weight state. We also have

$$L_n |h\rangle = 0, \quad n > 0. \quad (3.33)$$

From the highest weight state it is possible to create descendant states by acting on $L_{-k}, k > 0$ as

$$|h; k_1, k_2, \dots, k_n\rangle := L_{-k_1} L_{-k_2} \dots L_{-k_n} |h\rangle, \quad k_1 \leq k_2 \leq \dots \leq k_n. \quad (3.34)$$

We have

$$L_0 |h; k_1, k_2, \dots, k_n\rangle = (h + N) |h\rangle, \quad N = \sum_{i=1}^n k_i, \quad (3.35)$$

here N is the level of the state. These levels are degenerate as can be seen from the first few levels

$$\underbrace{L_{-1} |h\rangle}_{N=1}; \quad \underbrace{L_{-2} |h\rangle, L_{-1}^2 |h\rangle}_{N=2}; \quad \underbrace{L_{-3} |h\rangle, L_{-2} L_{-1} |h\rangle, L_{-1}^3 |h\rangle}_{N=3}; \dots \quad (3.36)$$

In fact, the number of states $d(N)$ in level N is given by the partition of the integer N . Now, at a given level the linear combinations of base states can give rise to null states⁵ and it is necessary to remove these states. Moreover, if we want the CFT to be **unitary**, we also need to remove the negative norm states. This imposes various constraints on the CFT central charge c and the content of highest weight representations h associated with it and in particular, tell us when a *unitary* representation is allowed to exist. The results are [3]

- For $c > 1$, $h > 0$ unitary representations can exist.
- For $c = 1$ unitary representations are disallowed for $h = \frac{n^2}{4}$, $n \in \mathbb{Z}$
- For $c < 1$ and $h \geq 0$ unitary representations are allowed for the following discrete values of c and corresponding highest weight representations $h_{p,q}$

$$\begin{aligned} c &= 1 - \frac{6}{m(m+1)}; \quad m = 3, 4, \dots \\ h_{p,q} &= \frac{((m+1)p - mq)^2 - 1}{4m(m+1)}; \quad 1 \leq p \leq m-1, 1 \leq q \leq m. \end{aligned} \tag{3.37}$$

CFTs with discrete c and finite number of highest weight representations are called Rational CFT (RCFT).

Similarly, we can repeat our analysis for the anti-holomorphic part of the algebra and build a positive norm representation for it. Since the holomorphic and anti-holomorphic parts commute the total Hilbert space takes the form

$$\mathcal{H} \equiv V(c, h) \otimes \bar{V}(\bar{c}, \bar{h}). \tag{3.38}$$

3.2.3 Torus Partition Function

So far we have been working on a radial quantized picture where the theory is defined on a cylinder of circumference 2π and time runs along the length of the cylinder. The prescription of calculating the partition

⁵In order to compute the norm, one defines the conjugation operation as $L_m^\dagger = L_{-m}$.

3.2. CFT in $d = 2$ dimensions

function path integral formalism of QFT involves considering trajectories periodic in time. If we compactify the time direction as $t \sim t + 1$, the cylinder becomes a torus. Before we discuss the CFT on a torus, let us discuss some general properties of a torus in the complex plane. Most of the discussion in this section closely follows [25].

The complex torus can be obtained from a lattice in complex plane by the following equivalence relation

$$z \equiv z + nw_1 + mw_2, \quad n, m \in \mathbb{Z}, \quad (3.39)$$

where (w_1, w_2) are complex numbers called the periods of the lattice. Without the loss of generality we can take $\text{Im}(w_2/w_1) > 0$.

Claim 1. Suppose (w'_1, w'_2) are two other periods related to (w_1, w_2) by

$$\begin{pmatrix} w'_1 \\ w'_2 \end{pmatrix} = \begin{pmatrix} a & b \\ c & d \end{pmatrix} \begin{pmatrix} w_1 \\ w_2 \end{pmatrix}; \quad ad - bc = 1, \quad a, b, c, d \in \mathbb{Z}. \quad (3.40)$$

Then, these two sets of periods describe the same torus.

Proof. Since (w'_1, w'_2) is expressed as a linear combination of (w_1, w_2) , they describe the same lattice. Inverting the relation

$$\begin{pmatrix} w_1 \\ w_2 \end{pmatrix} = \begin{pmatrix} d & -b \\ -c & a \end{pmatrix} \begin{pmatrix} w'_1 \\ w'_2 \end{pmatrix}; \quad a, b, c, d \in \mathbb{Z}. \quad (3.41)$$

This implies that (w_1, w_2) is in the same lattice as (w'_1, w'_2) . □

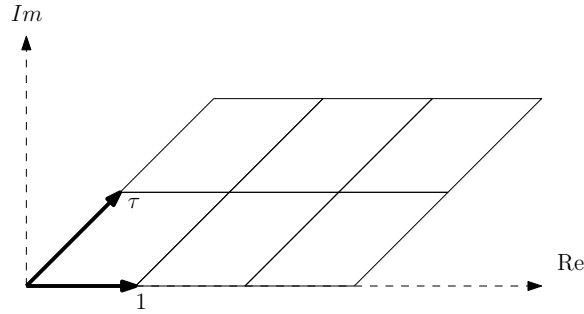


Figure 3.3: Torus in the complex plane whose periods are chosen to be 1 and τ .

3.2. CFT in $d = 2$ dimensions

It can be shown that in the complex plane two lattices are equal if they differ by a rotation and scaling factor [26]. We can use this freedom to take (w_1, w_2) in the form $(1, \tau)$ with $\text{Im } \tau > 0$ and choose the vertices of the lattice to be $(0, 1, \tau, 1 + \tau)$, τ is called the modular parameter of the lattice (fig. 3.3). We must have the lattice to be invariant under

$$\tau \rightarrow \frac{a\tau + b}{c\tau + d}, \quad ad - bc = 1 \quad (3.42)$$

The above relation is called the modular transformation and the transformation group is known called $SL(2, \mathbb{Z})/\mathbb{Z}_2$.⁶ It can be shown that any matrix $\begin{pmatrix} a & b \\ c & d \end{pmatrix}$ can be obtained by multiplying the following two matrices to appropriate powers

$$T = \begin{pmatrix} 1 & 0 \\ 1 & 1 \end{pmatrix}, \quad S = \begin{pmatrix} 0 & 1 \\ -1 & 0 \end{pmatrix}. \quad (3.43)$$

These are the generators of the $SL(2, \mathbb{Z})/\mathbb{Z}_2$ group. This poses a physical restriction on CFTs on a torus namely, *any physical quantity on the torus should be invariant under the modular S and T transformations.*

Now, let us take our “time” axis to be $\text{Im}(\tau)$ and the space axis to be the real line. It can be easily seen from figure 3.3, the $(0, 0)$ point does not get mapped to itself if we compactify in the “time” direction. Additionally, we need to twist by an amount $\text{Re}(\tau)$ to the *left*. Thus we define the partition function on a torus as

$$Z := \text{Tr } e^{-2\pi \text{Im}(\tau)H + 2\pi \text{Re}(\tau)P}, \quad (3.44)$$

where H and P generate translations in time and space directions respectively. Thus they simply correspond to the Hamiltonian and momentum. It is easy to write down the expression for the Hamiltonian on a cylinder of circumference 2π :

$$\begin{aligned} H &= \frac{1}{2\pi} \int_0^{2\pi} d\sigma T_{tt}(\sigma) \\ &= \frac{1}{2\pi} \int_0^{2\pi} d\sigma (T(\sigma) + \bar{T}(\sigma)) \\ &= L_0 + \bar{L}_0 - \frac{c}{12}. \end{aligned} \quad (3.45)$$

⁶Changing the signs of all a, b, c, d does not affect the modular transformation formula, this is the origin of \mathbb{Z}_2 quotient.

3.2. CFT in $d = 2$ dimensions

To derive this relation we have used the fact that the coordinates in the cylinder $w = t + i\sigma$ are mapped to the plane by $w = \ln z$. In the second line, we have used (3.14) and finally, in the third line, we have used (3.25) to go from the cylinder to the complex plane. Similarly, we obtain for the momentum operator on the cylinder,

$$\begin{aligned} P &= \frac{1}{2\pi} \int_0^{2\pi} \int d\sigma T_{t\sigma}(\sigma) \\ &= i(L_0 - \bar{L}_0). \end{aligned} \quad (3.46)$$

Substituting in the definition of the partition function (3.44) gives

$$Z(\tau, \bar{\tau}) = \text{Tr}_{\mathcal{H}} \left(q^{L_0 - c/24} \bar{q}^{\bar{L}_0 - c/24} \right) \quad (3.47)$$

where $q = e^{2\pi i\tau}$, $\bar{q} = e^{2\pi i\bar{\tau}}$ and the trace is taken over the Hilbert space of the theory (3.38). Since the Hilbert space is a direct product of the holomorphic and anti-holomorphic part of the theory. The partition function takes the form

$$Z(\tau, \bar{\tau}) = \sum_{h, \bar{h}} \chi_h(\tau) \chi_{\bar{h}}(\bar{\tau}) \quad (3.48)$$

where $\chi_h(\tau) = q^{c/24} \text{Tr}_h q^{L_0}$ is called the **character** and the trace is taken over the sector with highest weight field of conformal dimension h and it's descendants.

As mentioned above, the theory on a torus must respect T and S transformations. Under T and S the modular parameter τ transforms as $T : \tau \rightarrow \tau + 1$ and $S : \tau \rightarrow -\frac{1}{\tau}$. So we must have

$$\begin{aligned} Z(\tau + 1) &= Z(\tau) \\ Z\left(-\frac{1}{\tau}\right) &= Z(\tau), \end{aligned}$$

and similar for the antiholomorphic part. We finish this section by noting some properties of the character under T and S ;

$$T : \chi_h(\tau + 1) = e^{2\pi i(h - c/24)} \chi_h(\tau). \quad (3.49)$$

The transformation under S is not so trivial. It takes the form

$$S : \chi_h(-1/\tau) = \sum_k S_{hk} \chi_k(\tau). \quad (3.50)$$

The matrix S_{hk} is called modular S -matrix.

3.3 Boundary Conformal Field Theory

In this section, we will discuss the basics of conformal field theory with a planar boundary in $d = 2$ dimension. The generalization to $d \geq 3$ is non-trivial and in general is much harder. A canonical reference for BCFT in general d is [24].

3.3.1 The Doubling Trick

Let us take our CFT to be defined in the upper half plane $\text{Im}(z) \geq 0$ with the boundary being the real axis $\text{Im}(z) = 0$. This means all our operators and fields are only defined on the upper half plane. We shall denote such quantities with a superscript (H) . We must impose some boundary condition on the operators of the theory. One natural choice is to take

$$T_{01}^{(H)} = 0 = T_{10}^{(H)}, \quad x^0 = 0 \quad (3.51)$$

This condition is often referred as the conformal boundary condition. The physical meaning of (3.51) is that no energy or momentum flows across the boundary. In complex coordinate, this condition becomes

$$T^{(H)}(z) = \bar{T}^{(H)}(\bar{z}), \quad z = \bar{z}. \quad (3.52)$$

Eq. (3.51) motivates the formulation of so-called method of images. In CFT, the variation of a local field was written in terms of the stress tensor in (3.18) which we repeat here for convenience

$$\delta\phi(w, \bar{w}) = \frac{1}{2\pi i} \left(\oint_C dz f(z) R(T(z)\phi(w, \bar{w})) - \oint_{\bar{C}} d\bar{z} \bar{f}(\bar{z}) R(\bar{T}(\bar{z})\phi(w, \bar{w})) \right) \quad (3.53)$$

We can write down analogous relation for CFT in upper half-plane except the contours are taken to be semi-circles instead of circles centering the origin and all fields are defined in the upper half-plane. Additionally, unlike the theory in the full plane, $\bar{f}(\bar{z})$ is now the complex conjugate of $f(z)$ since only these types of transformations leave the real line invariant. Thus again, we find that the anti-holomorphic and holomorphic degrees are coupled. First, (3.52) suggests an analytic continuation of the stress tensor in the lower half-plane. To this end we define a new *chiral* energy-momentum tensor in the *full* complex plane

$$T(z) := \begin{cases} T^{(H)}(z) & \text{for } \text{Im}(z) > 0 \\ \bar{T}^{(H)}(z) & \text{for } \text{Im}(z) < 0 \end{cases} \quad (3.54)$$

3.3. Boundary Conformal Field Theory

We also define a mirror image of the field in the lower half-plane identifying it with the anti-holomorphic part of the field as shown in 3.4. The \bar{z} dependence of the fields are treated to be the dependence in the holomorphic coordinate $\bar{z} = z^*$ in the lower half-plane.

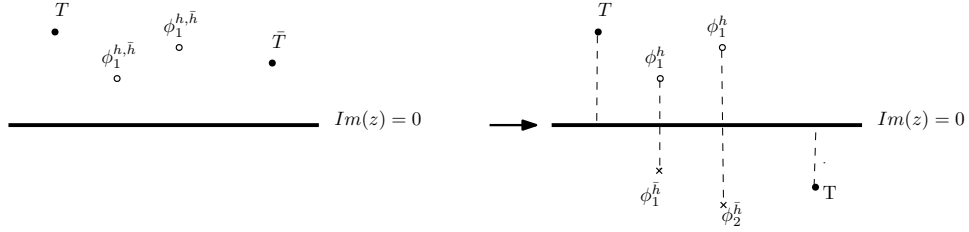


Figure 3.4: Using the doubling trick, the theory in the upper half plane can be mapped to a theory defined on the full plane.

This is known as the doubling trick in analogy with the method of images in electrostatics. Using this the semi-circle integration contours can be deformed to circular contours in the full plane as shown in figure 3.5:

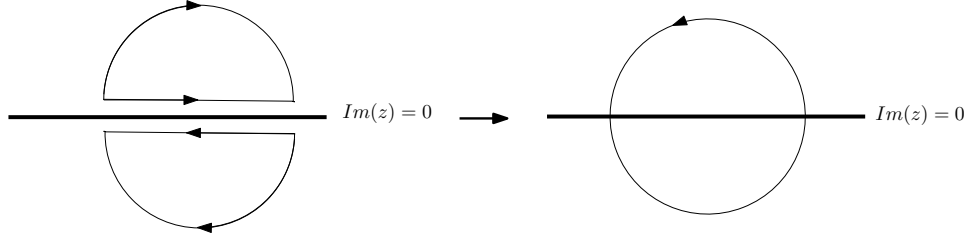


Figure 3.5: Using doubling trick the semi-circular integration contours in upper half plane can be deformed to a circular contour in full plane. On the real line the contributions from each semi-circle cancel due to (3.51).

In the radial quantization picture, we can also define the dilatation operator

$$D := \frac{1}{2\pi i} \oint_S dz z T^H(z) - \frac{1}{2\pi i} \oint_{\bar{S}} d\bar{z} \bar{z} \bar{T}^H(\bar{z}) = \frac{1}{2\pi i} \oint_C dz z T(z) L \quad (3.55)$$

and analogously other modes

$$L_n = \frac{1}{2\pi i} \oint_C dz z^{n+1} T(z) \quad (3.56)$$

However, we emphasize the fact that $T(z)$ is analytic in z so there is just one set of Virasoro algebra

$$[L_m, L_n] = (n - m)L_{m+n} + \frac{c}{12}m(m^2 - 1)\delta_{m+n,0}. \quad (3.57)$$

3.3.2 Cardy's Condition

A unique feature of any QFT with a boundary is the existence of the boundary states. In the context of 2d CFTs boundary states originates from two equivalent descriptions of the same theory. However, these boundary states are unique in the sense that they are subjected to a strong consistency condition known as the Cardy's condition [6, 7].

Let's start by computing the annulus partition function. We start with an infinite strip of width L and take the time direction to be running along the length of the strip. If we take a periodic path of circumference T in time, we obtain the annulus geometry with boundary condition (a, b) on both sides (see fig 3.6).

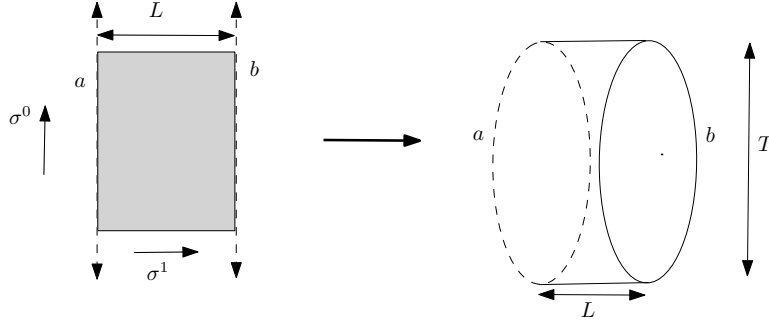


Figure 3.6: With a periodic trajectory in σ^0 direction, the infinite strip becomes a cylinder with boundary conditions a and b on each side.

To compute the partition function, we map the infinite strip to the upper half-plane by

$$z = e^{\frac{\pi}{L}}(\sigma_0 + i\sigma), \quad (3.58)$$

where (σ_0, σ_1) are the coordinates on the annulus and z is the coordinate on the upper half plane. The Hamiltonian can be computed

using (3.25) to be

$$H_{ab} = \frac{\pi}{L} \left(L_0 - \frac{c}{24} \right) \quad (3.59)$$

Now in analogy with in CFT in torus, we can define a partition function as

$$\begin{aligned} Z_{ab}^{open} &= \text{Tr} e^{-TH_{ab}} \\ &= \text{Tr} e^{-\frac{\pi T}{L}((L_0)_{ab} - \frac{c}{24})}; \quad q = 2\pi i\tau; \quad \tau = \frac{iT}{2L} \\ &= \sum_h N_{ab}^h \chi_h(q) \end{aligned} \quad (3.60)$$

Notice that we only have one set of oscillator as expected for a BCFT. In the final expression we expanded the partition function as a linear combination of the chiral character. The number N_{ab}^h denotes how many times the character h appears when with a particular boundary condition (a, b) . In particular, a vacuum can appear only when the boundary conditions are the same on both sides and it appears only once. So we must have $N_{ab}^0 \delta_{ab} = 1$. The partition function (3.60) of often called the open string partition function.

However, since we are working in the Euclidean signature, we are allowed to swap the role of time and space direction. In particular, the annulus partition function can be view as the transition amplitude of a CFT defined on a circle of circumference T being emitted from a ‘boundary state’ $|a\rangle$ and being absorbed in a boundary state $|b\rangle$ after a time π . CFT on a circle can be mapped to the plane by a conformal mapping

$$z = e^{-\frac{2\pi}{T}(\sigma_0 + i\sigma_1)}. \quad (3.61)$$

Notice we have swapped the role of space and time. Again, using this map we can compute the Hamiltonian on the circle

$$H = \frac{2\pi}{T} \left(L_0 + \bar{L}_0 - \frac{c}{12} \right) \quad (3.62)$$

The propagation amplitude from a to b reads

$$\begin{aligned}
 Z_{ab,closed} &= \langle a | e^{LH'} | b \rangle \\
 &= \langle a | e^{-L\frac{2\pi}{T}(L_0 + \bar{L}_0 - \frac{c}{12})} | b \rangle \\
 &= \langle a | e^{-L\frac{2\pi}{T}(L_0 + \bar{L}_0 - \frac{c}{12})} | b \rangle \\
 &= \langle a | \tilde{q}^{\frac{1}{2}(L_0 + \bar{L}_0 - \frac{c}{12})} | b \rangle; \quad \tilde{q} = \frac{-2\pi i}{\tau}. \quad (3.63)
 \end{aligned}$$

We also need to ensure the conformal boundary condition (3.51) on each side of the cylinder. In terms of the Laurent modes of the stress tensor it reads

$$L_n - \bar{L}_{-n} = 0 \quad (3.64)$$

Thus the boundary states must satisfy

$$(L_n - \bar{L}_{-n}) | a \rangle = 0, \quad (L_n - \bar{L}_{-n}) | b \rangle = 0. \quad (3.65)$$

The solution to (3.65) is given by Ishibashi states [17]. They are a subspace of $V_{c,h} \otimes \bar{V}_{\bar{c},\bar{h}}$ that can be written in the form

$$|h\rangle\rangle = \sum_N |h, N\rangle \otimes \overline{|h, N\rangle}. \quad (3.66)$$

Here $|h, N\rangle$ denotes a state in the highest weight representation h . In the anti-holomorphic sector it is paired with the same basis state $\overline{|h, N\rangle}$. The boundary states can be written as a linear combination of Ishibashi states i.e

$$|a\rangle = \sum_h \langle\langle h|a\rangle\rangle |h\rangle\rangle \equiv \sum_h a_h |h\rangle\rangle \quad (3.67)$$

Using this definition we compute the overlap function

$$\begin{aligned}
 Z_{ab}^{closed} &= \sum_h a_h^* b_h \chi_h(\tilde{q}) \\
 &= \sum_{h,k} a_h^* b_h S_k^h \chi_k(q) \quad (3.68)
 \end{aligned}$$

In the last line we have performed a modular S -transform. However, this overlap is exactly equal to the annulus partition function⁷. Comparing

⁷This is often called the open string-closed string duality.

3.3. Boundary Conformal Field Theory

with (3.60) we obtain a condition for the coefficients a_h, b_h :

$$\sum_k a_k^* b_k S_k^h = N_{ab}^h. \quad (3.69)$$

This is a very strong condition in the sense that the number N_{ab}^h is an integer. This condition is called Cardy's condition.

For RCFTs Cardy gave a solution to (3.69). If the coefficients are chosen such that

$$a_h = \frac{S_{ah}}{\sqrt{S_{0h}}} \quad (3.70)$$

Then (3.69) reads

$$\sum_k \frac{S_{ak} S_{bk} S_{kh}}{S_{0k}} = N_{ab}^h. \quad (3.71)$$

For RCFT the above relation is always true due to an identity called the Verlinde formula [37].

One particular quantity that will later become important in our analysis is called the boundary entropy. In the limit $\tau \rightarrow 0$ the dominant term in (3.63) is the vacuum sector $h = 0$. Consequently

$$Z_{ab, \text{closed}} \approx \langle a|0\rangle \langle b|0\rangle e^{-\frac{\pi cL}{6T}}. \quad (3.72)$$

From this we can define the free energy $F_{ab} = -T^{-1} \ln Z_{ab}$ to compute the entropy

$$S_{ab} = \frac{\pi cL}{3T} + g_a + g_b \quad (3.73)$$

where $g_a = \ln \langle a|0\rangle$, $g_b = \ln \langle b|0\rangle$ are called the **boundary entropy**.

Chapter 4

Symmetric Orbifold BCFT

In the last chapter, we have discussed the basics of boundary conformal field theory (BCFT) in two dimensions. In particular, we have discussed Cardy's condition which imposes a non-trivial condition on the boundary states. In this section, we shall generalize this construction for symmetric orbifold BCFTs. In section 4.1 we discuss the role of symmetric orbifold CFT in the context of AdS/CFT. Next in section 4.2 we discuss the AdS/BCFT correspondence to motivate our study of large- N orbifold BCFTs. Finally, in section 4.3, we construct the Cardy consistent boundary states for symmetric BCFT and comment on its holographic implications.

4.1 AdS/CFT Correspondence and Symmetric Orbifold

The AdS/CFT correspondence [23] states that quantum gravity in Anti de-Sitter spacetime in $d + 1$ dimensions is exactly equivalent to a d dimensional CFT. An important question is that what CFTs describe semi-classical gravity in the bulk [16]. In AdS_3/CFT_2 the first hint in answering this question comes from the Brown-Henneaux formula [4] relating the CFT central charge c to the gravity data as

$$c = \frac{3l_{AdS}}{2G_N}. \quad (4.1)$$

Here l_{AdS} is the AdS radius and G_N denotes the Newton's constant. In the semi-classical limit $G_N \ll 1$, this implies that the corresponding CFT should have a large central charge $c \gg 1$. However, CFTs with large c are not thoroughly understood.

One easy way to construct a CFT with a large central charge is as follows: take the N copies of your favorite CFT \mathcal{C} and take the N -fold

tensor product $\mathcal{C}^{\otimes N}$. The product theory has S_N invariance under the labeling of the seed theory. So we mod out by the symmetry group S_N and construct the symmetric orbifold theory

$$\mathcal{C}^{\otimes N}/S_N. \quad (4.2)$$

This theory has central charge $c_{eff} = Nc$, where c is the central charge of the seed theory. In the large N limit we have $c_{eff} \gg 1$. Indeed, large- N symmetric orbifold CFT captures many features of the semi-classical gravity theory [2, 21] and has been studied extensively in this context. We refer to the reader to the references listed in [1, 31].

Apart from their relevance to holography, symmetric orbifold CFTs are interesting in their own right. Consider, N scalars theory $X^I(z)$ with $I = 1, 2, \dots, N$. If we only had one copy, we would have $X(e^{2\pi i}z) = X(z)$. However, since the theory is invariant under permutation of the indices I , we can have

$$X^I(e^{2\pi i}z) = X^{\sigma(I)}(z), \quad \sigma \in S_N. \quad (4.3)$$

The mapping (4.3) gives rise to new states in the theory called the twisted sector states. The cycle decomposition of an element $g \in S_N$

$$g = (1)^{m_1}(2)^{m_2} \dots (N)^{m_N}; \quad \sum_k km_k = N, \quad (4.4)$$

makes it possible to build the Hilbert space of the S_N orbifold out of the \mathbb{Z}_n orbifolds [31] where n is a cycle of length n in the cycle decomposition of $g \in S_N$. In the twisted sector of the \mathbb{Z}_n orbifold, the fractional Virasoro modes are defined as [5]

$$L_{-m/k} = \oint \frac{dz}{2\pi i} \sum_{j=1}^N T^j(z) e^{-2\pi i(j-1)/k} z^{1-m/k}. \quad (4.5)$$

These modes satisfy the algebra

$$\left[L_{\frac{n}{k}}, L_{\frac{n'}{k}} \right] = \frac{n-n'}{k} L_{\frac{n+n'}{k}} + \delta_{n+n',0} \frac{c}{12} \left(\left(\frac{n}{k} \right)^2 - 1 \right) \frac{n}{k}. \quad (4.6)$$

These fractional modes give rise to new twisted primaries. For example, the lowest twisted primary has conformal dimension [22]

$$h_{twisted,0} = \frac{c}{24} \frac{n^2 - 1}{n}. \quad (4.7)$$

The twist operators have very non-trivial correlation functions and other interesting properties [5, 9, 31]. Although much is known about symmetric orbifold CFTs, the case of symmetric orbifold BCFTs has not been studied yet. In this chapter, we shall make the first attempt to understand some aspects of symmetric product BCFTs. But before that, let us comment on the relevance of BCFTs to holography, which is the topic of the next section.

4.2 AdS/BCFT Correspondence

In analogy with AdS/CFT correspondence, we can also talk about the holographic dual of BCFT. The general setup is as follows [36]. Consider a CFT defined on a d dimensional manifold M with boundary ∂M . The dual AdS geometry is given by a $d+1$ dimensional N manifold such that $\partial N = M \cup Q$ with Q being homologous to M fig 4.1. The gravity dual of the CFT manifold i.e Q is often referred to as a brane.

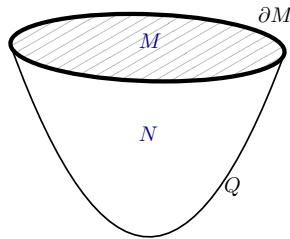


Figure 4.1: The CFT is defined on a manifold M with boundary ∂M . On the bulk the boundary ∂M extends to the boundary Q of the dual N of M such that $\partial N = M \cup Q$

If we consider the gravity dual of the half line, the location of the boundary depends on the tension of the brane in a particular way (fig 4.2)

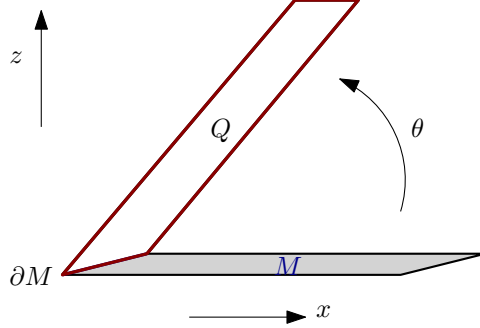


Figure 4.2: The gravity dual of half line. The location of the boundary $\rho = \rho^*$ depends on the brane tension via (4.8) and $\cot \theta = \sinh \frac{\rho^*}{l_{AdS}}$

On AdS_d foliation of AdS_{d+1} defined by [19]

$$ds_{AdS_{d+1}}^2 = d\rho^2 + \cosh^2 \left(\frac{\rho}{l_{AdS}} \right) ds_{AdS}^2 \quad (4.8)$$

the location of the brane at $\rho = \rho^*$ is related to the tension of the brane as [36]

$$T = \frac{d-1}{l_{AdS}} \tanh \frac{\rho^*}{l_{AdS}}. \quad (4.9)$$

Here

$$T_{ab} = \frac{2}{\sqrt{-h}} \frac{\delta I_Q}{\delta h_{ab}}. \quad (4.10)$$

and h_{ab} is the metric on the brane. We are considering constant T . In the case of when the brane is topologically equivalent to a disk, there is a relation between the BCFT boundary entropy and the brane tension given by

$$g_a = \frac{\rho^*}{4G_N} = \frac{c}{6} \operatorname{arctanh} \frac{T l_{AdS}}{d-1} \quad (4.11)$$

Thus we have discovered that a full characterization of boundary states should give us the boundary entropy which will, in turn, determine the location of the dual brane.

4.3 Boundary States in Symmetric Orbifold BCFT

In this section, we shall study the Cardy consistent boundary states in symmetric orbifold BCFT. As before we take N copies of BCFTs and consider $C^{\otimes N}/S_N$ orbifold. In section 4.3.1 we give an ansatz for Cardy consistent boundary states in symmetric BCFT. In the following two sections we discuss two examples illustrating and justifying our ansatz. Finally, in 4.3.4 we compute the boundary entropy in the large N limit.

4.3.1 Ansatz for Boundary State

Let us assume that each seed theory is equipped with a set of Cardy consistent boundary states. A “consistent” boundary state in the orbifold theory must satisfy the following two properties

- The transition amplitude between any two boundary states as in (3.63) has to be interpreted as a partition function in the open string channel. In particular, it can be written as a linear combination of chiral characters with integer coefficients.
- The vacuum channel appears only once.

Let’s denote a boundary state in the k -fold product theory using a permutation g and seed boundary state label b in the form $|b_g\rangle$. Here g is an element of S_N written in the cycle decomposition as

$$g = (1)^{m_1}(2)^{m_2}\dots(N)^{m_N}; \quad \sum_k km_k = N, \quad (4.12)$$

For example, the permutation

$$g = (1)(23) \quad (4.13)$$

and seed b denotes the state

$$|b_{(1)(23)}\rangle \equiv |b_{(1)}\rangle|b_{(23)}\rangle. \quad (4.14)$$

The elements that belong to the same cycle have to be twisted together. If the cycle length is n , the n -twisted boundary states $|a_{(n)}\rangle$ reads

$$|a_{(n)}\rangle = \sum_h a_h \left| \frac{h}{N} \right\rangle \rangle \quad (4.15)$$

and the Ishibashi states satisfy the twisted sector gluing condition

$$\left(L_{\frac{m}{n}} - \bar{L}_{-\frac{m}{n}} \right) \left| \frac{h}{n} \right\rangle \rangle = 0; \quad m \in \mathbb{N}. \quad (4.16)$$

We will denote the centralizer of g in the group S_k by $C_k(g)$. We can write the permutations of k consecutive integers $a+1, \dots, a+k$ as $S_k(a)$. So, for example

$$g = (4)(56) \quad (4.17)$$

is a permutation in $S_3(3)$.

We will denote multiplicities of seed states given by an integer valued vector $\vec{n} \in \mathbb{Z}_+^M$ where the seed theory has M boundary states, $b^{(i)}$, and $|\vec{n}| = N$. We can also write the partial sums $\sum_{j=1}^{i-1} n_j = N_i$

The conjecture for the general formula for the state:

$$|\vec{n}\rangle = \frac{1}{\sqrt{N!}} \sum_{h \in S_N} \prod_{i=1}^M \left(\frac{1}{n_i!} \sum_{g_i \in S_{n_i}(N_i)} |b_{hg_i h^{-1}}^i\rangle \right) \quad (4.18)$$

4.3.2 Example 1: $N = 2$

First, we have the situation when all seed theory boundary states are same. Formula (4.18) reads

$$|(2)\rangle = \frac{1}{\sqrt{2}} (|a\rangle |a\rangle + |a_{12}\rangle). \quad (4.19)$$

Here $|a\rangle$ is the Cardy consistent boundary state in the seed theory and we have defined the labeling $b^{(1)} \equiv a$. $|a_{(2)}\rangle$ is a state that is present in the twisted sector,

$$|a_{(2)}\rangle = \sum_h a_h \left| \frac{h}{2} \right\rangle \rangle; \quad h \in \mathcal{C}, \quad (4.20)$$

where \mathcal{C} denotes the seed theory. Note that the coefficients a_h in (4.20) are the same as in the seed theory. Explicitly, we write the orbifold Ishibashi states as

$$\left| \frac{h}{2} \right\rangle \rangle \equiv \sum_M \left| \frac{h}{2}, M \right\rangle \otimes \overline{\left| \frac{h}{2}, M \right\rangle} \quad (4.21)$$

In the above expression descendants M of the highest weight state $|h/2\rangle$ are produced by acting on the highest weight state $|\frac{h}{2}\rangle$ by fractional Virasoro modes $L_{-m/2}$. $|a\rangle_t$ satisfies the following gluing condition in the twisted sector

$$(L_{\frac{m}{2}} - \bar{L}_{-\frac{m}{2}}) \left| \left\langle \frac{h}{2} \right\rangle \right\rangle = 0. \quad (4.22)$$

The overlap of two such states $\langle (2)_a | \tilde{q} | (2)_b \rangle$ in the closed string channel reads as follows in the open string channel

$$Z_{ab}^{open} = \frac{1}{2} (Z_{ab}^2(\tau) + Z_{ab}(2\tau)). \quad (4.23)$$

The above expression has integer coefficients for all characters appearing in the open string partition function.

Next we consider the condition when the condition on the seed theories are different $b^{(1)} \equiv a$, $b^{(2)} \equiv b$. Our ansatz gives

$$|(1, 1)_{ab}\rangle = \frac{1}{\sqrt{2}} (|a\rangle |b\rangle + |b\rangle |a\rangle) \quad (4.24)$$

In the open string channel the overlap $\langle (1, 1)_{ab} | \tilde{q} | (1, 1)_{cd} \rangle$ reads

$$Z_{ab,cd}^{open} = Z_{ac}(\tau)Z_{bd}(\tau) + Z_{ad}(\tau)Z_{bc}(\tau). \quad (4.25)$$

This shows as long as $a \neq b$, the above overlap can be interpreted as a partition function. Finally, we note that the following overlap $\langle (1, 1)_{ab} | \tilde{q} | (2)_c \rangle$ is also a partition function in the open string channel, namely

$$Z_{ab,c}^{open} = Z_{ac}(\tau)Z_{bc}(\tau). \quad (4.26)$$

4.3.3 Example 2: $N = 3$

Let us consider the case when all three seed theory states have same boundary condition, say a . We have

$$\begin{aligned} |(3)\rangle &= \frac{1}{\sqrt{6}} (|a_1\rangle |a_2\rangle |a_3\rangle + |a_1\rangle |a_{(23)}\rangle + |a_2\rangle |a_{(13)}\rangle + |a_3\rangle |a_{(12)}\rangle \\ &\quad + |a_{(123)}\rangle + |a_{(132)}\rangle) \end{aligned} \quad (4.27)$$

The overlap of two such states $\langle (3)_a | \tilde{q} | (3)_b \rangle$ reads in the open string channel

$$Z_{a,b}^{open} = \frac{1}{6} Z_{ab}^3(\tau) + \frac{1}{2} Z_{ab}(\tau) Z_{ab}(2\tau) + \frac{1}{3} Z_{ab}(3\tau). \quad (4.28)$$

Next, we consider the case when two indices that label the boundary condition in each theory are same. We have from our general ansatz

$$\begin{aligned} |(2)_a, (1)_b \rangle &= \frac{1}{\sqrt{6}} (|a_1\rangle |a_2\rangle |b_3\rangle + |a_1\rangle |b_2\rangle |a_3\rangle + |b_1\rangle |a_2\rangle |a_3\rangle \\ &\quad + |b_1\rangle |a_{(23)}\rangle + |b_2\rangle |a_{(13)}\rangle + |b_3\rangle |a_{(12)}\rangle) \end{aligned} \quad (4.29)$$

The overlap $\langle (2)_c | \tilde{q} | (2)_a, (1)_b \rangle$ reads in the open string channel

$$Z_{aab,c}^{open} = \frac{1}{2} [Z_{ac}^2(\tau) + Z_{ac}(2\tau)] Z_{bc}(\tau) \quad (4.30)$$

and its overlap with itself reads

$$Z_{aab,cdd}^{open} = Z_{ac}(\tau) Z_{bc}(\tau) Z_{ad}(\tau) + \frac{1}{2} [Z_{ac}^2(\tau) + Z_{ac}(2\tau)] Z_{bd}(\tau) \quad (4.31)$$

Next we consider the case when all three indices are different. In this case we have

$$\begin{aligned} |(1)_a, (1)_b, (1)_c \rangle &= \frac{1}{\sqrt{6}} (|a_1\rangle |b_2\rangle |c_3\rangle + |b_1\rangle |c_2\rangle |a_3\rangle + |c_1\rangle |a_2\rangle |b_3\rangle \\ &\quad + |a_1\rangle |c_2\rangle |b_3\rangle + |c_1\rangle |b_2\rangle |a_3\rangle + |b_1\rangle |a_2\rangle |c_3\rangle) \end{aligned} \quad (4.32)$$

The overlap $\langle (3)_c | \tilde{q} | (1)_a, (1)_b, (1)_c \rangle$ takes the form

$$\tilde{Z}_{open}^{abc,d} = Z_{ad}(\tau) Z_{bd}(\tau) Z_{cd}(\tau) \quad (4.33)$$

Similarly, the overlap $\langle (1)_a, (1)_b, (1)_c | \tilde{q} | (2)_p, (1)_q \rangle$ reads

$$\tilde{Z}_{open}^{abc,pq} = Z_{ap}(\tau) Z_{bp}(\tau) Z_{cq}(\tau) + Z_{aq}(\tau) Z_{bp}(\tau) Z_{cp}(\tau) + Z_{ap}(\tau) Z_{bq}(\tau) Z_{cp}(\tau). \quad (4.34)$$

Finally, it's overlap with itself $\langle (1)_a, (1)_b, (1)_c | \tilde{q} | (1)_p, (1)_q, (1)_r \rangle$ is

$$\begin{aligned} \tilde{Z}_{open}^{abc,pqr} &= Z_{ap}(\tau) [Z_{bq}(\tau) Z_{cr} + Z_{br}(\tau) Z_{cq}(\tau)] \\ &\quad + Z_{bp}(\tau) [Z_{ar}(\tau) Z_{cq} + Z_{aq}(\tau) Z_{cr}(\tau)] \\ &\quad + Z_{cp}(\tau) [Z_{aq}(\tau) Z_{br} + Z_{ar}(\tau) Z_{bq}(\tau)] \end{aligned} \quad (4.35)$$

which are all perfectly fine partition functions.

4.3.4 Boundary Entropy and Brane Spectrum

The boundary entropy is given by the vacuum overlap $g_{\vec{n}} = \ln \langle \vec{n} | 0 \rangle$ in the closed string channel. However, the twisted sector has zero overlap with $|0\rangle$ since the twisted vacuum has higher energy due to the existence of the fractional modes (see (4.7)). This observation enormously simplifies the computation of boundary entropy. In particular, only the untwisted sectors given by $g_i = (id)_i$ in (4.18) contribute to $g_{\vec{n}}$. We have,

$$g_{\vec{n}} = \ln \left[\frac{1}{\sqrt{N!}} \sum_{h \in S_N} \prod_{i=1}^M \left(\frac{1}{|S_{n_i}(N_i)|} \langle b_{h^{(i)} h^{-1}}^{(i)} | 0 \rangle \right) \right]. \quad (4.36)$$

In our example of $N = 3$ we have

$$\begin{aligned} g_{(3)} &= 3g_a - \frac{1}{2} \ln 6, \\ g_{(2),(1)} &= \ln [3(2\langle a|0\rangle + \langle b|0\rangle)] - \frac{1}{2} \ln 6, \\ g_{(1),(1),(1)} &= \ln [6(\langle a|0\rangle + \langle b|0\rangle) + \langle c|0\rangle] - \frac{1}{2} \ln 6 \end{aligned} \quad (4.37)$$

Next, we concentrate on the large N limit.

Planckian branes

Here, we discuss how to obtain branes with a tension that scales *linearly* with N . Consider the boundary state with \sqrt{N} different boundary states of the seed theory. The relevant term of the boundary state to compute the overlap with the vacuum is

$$\frac{1}{\sqrt{N!}} \sum_g \frac{1}{(\sqrt{N!})^{\sqrt{N}}} g |a^1\rangle^{\sqrt{N}} \dots |a^{\sqrt{N}}\rangle^{\sqrt{N}}. \quad (4.38)$$

To understand the combinatorical factor, we sum over all elements of the group, that is the $N!$ upstairs, but we then divide by the permutations that didn't do anything to the states. Those are the $\sqrt{N}!$ products

of $S_{\sqrt{N}}$. The boundary entropy is

$$\begin{aligned} \log \langle 0 | \frac{1}{\sqrt{N!}} \sum_g \frac{1}{(\sqrt{N!})^{\sqrt{N}}} g |a^1\rangle^{\sqrt{N}} \dots |a^{\sqrt{N}}\rangle^{\sqrt{N}} \\ = \log \frac{\sqrt{N!}}{(\sqrt{N!})^{\sqrt{N}}} + \log \left[\langle 0|a_1|0|a_1\rangle^{\sqrt{N}} \dots \langle 0|a^{\sqrt{N}}|0|a^{\sqrt{N}}\rangle^{\sqrt{N}} \right] \end{aligned} \quad (4.39)$$

which gives

$$g_{\text{full}} = \sqrt{N} \sum_{i=1}^{\sqrt{N}} g_i + \frac{N}{2}. \quad (4.40)$$

where we have used Stirling's approximation. Note that both terms are $\mathcal{O}(N)$, so we can have a tension of either sign. It's interesting though that there is this "bias" of $N/2$.

Super-Planckian branes

Next, we discuss the boundary states that give rise to branes with a tension scaling like $N \ln N$. These branes can be obtained from the states with labeling $g_{(N)}$ and $\underbrace{g_{(1), (1), \dots, (1)}}_N$ i.e. when all the seed

theory boundary conditions are same and all different respectively. The boundary entropy take the simple form

$$\begin{aligned} g_{(N)} &= N g_a - \frac{1}{2} \ln N! \\ \underbrace{g_{(1), (1), \dots, (1)}}_N &= \ln \left(N! \prod_{i=1}^N (\langle a_i | 0 \rangle) \right) - \frac{1}{2} \ln N! \end{aligned} \quad (4.41)$$

In the limit $N \gg 1$ this simplifies to

$$\begin{aligned} g_{(N)} &\approx N \left(g_a + \frac{1}{2} \right) - \frac{1}{2} N \ln N \\ &\approx -\frac{1}{2} N \ln N \end{aligned} \quad (4.42)$$

$$\begin{aligned} \underbrace{g_{(1), (1), \dots, (1)}}_N &= \frac{1}{2} \ln N! + -\frac{N}{2} + \sum_{i=1}^N g_i \\ &\approx \frac{1}{2} N \ln N. \end{aligned} \quad (4.43)$$

Thus we find that the boundary entropy can go from negative to positive value corresponding to negative and positive tension branes⁸ Note that for non-minimal CFT, we have an infinite number of boundary states. Hence, the “typical” tension of the brane is determined by 4.43.

We have shown that a class of Cardy consistent boundary states can be constructed in symmetric orbifold BCFT from the data of seed theory boundary states. Before concluding this section, let us comment on other possibilities. Note that the boundary states have support on the twisted sector of the closed string. Also, the open string partition functions obtained in the examples (e.g. (4.28)) include the partition function of the *untwisted* sector of symmetric orbifold CFTs [2]. This has the following natural interpretation. In the symmetric product BCFT, the modular invariance is lost because of the unequal treatment of the space and time direction. If we want to evaluate the orbifold open string partition, we need to integrate over fields that have the following twist only in the time direction $X(z + \tau) = hX(z)$, $h \in S_N$. In the closed string channel, this twist by h acts on the space direction. Thus the resulting states have support on twisted the Hilbert space.

In our derivation, we have not imposed any structure on the seed theory. In particular, if the seed theory has additional structure there might be additional Cardy consistent boundary states. An example is the product theory of minimal model seed theory. It was shown in [30] that allowing permutation symmetry in seed theory gluing condition, it is possible to construct additional Cardy consistent boundary state. In that sense, our construction is simpler. It will be interesting to investigate the same problem when additional symmetries are permitted.

⁸Negative tension branes are non-fluctuating as argued in[19].

Chapter 5

Conclusion

In this thesis, we have studied two examples of boundary quantum field theory. In the first, example, we argued the zigzag edge of a semi-infinite graphene sheet should exhibit ferromagnetic order. A future work in this direction would be to study the other boundary condition known as the armchair edge in detail. The QFT in that scenario will be subjected to the so-called bag boundary condition [8]. One can introduce a four-fermi interaction in the bulk and investigate whether any non-trivial fixed point occurs in this theory.

In the second part of the thesis, we have constructed Cardy consistent boundary states in symmetric product BCFT. One interesting structure of these boundary states is that they are a mixture of the twisted and untwisted sector. Since this theory has a boundary one should have boundary localized twist operators appearing in the bulk-boundary OPE. These boundary twist operators are non-local and it will be very interesting to investigate their properties in detail. We leave these proposals for future work.

Bibliography

- [1] A. Belin, A. Castro, C. A. Keller, and B. Mühlmann. The holographic landscape of symmetric product orbifolds. *Journal of High Energy Physics*, 2020(1):1–28, 2020.
- [2] A. Belin, C. A. Keller, and A. Maloney. String universality for permutation orbifolds. *Physical Review D*, 91(10):106005, 2015.
- [3] R. Blumenhagen and E. Plauschinn. *Introduction to conformal field theory: with applications to string theory*, volume 779. Springer Science & Business Media, 2009.
- [4] J. D. Brown and M. Henneaux. Central charges in the canonical realization of asymptotic symmetries: an example from three dimensional gravity. *Communications in Mathematical Physics*, 104(2):207–226, 1986.
- [5] B. A. Burrington, I. T. Jardine, and A. W. Peet. The ope of bare twist operators in bosonic sn orbifold cfts at large n. *Journal of High Energy Physics*, 2018(8):1–31, 2018.
- [6] J. Cardy. Boundary conformal field theory. *arXiv preprint hep-th/0411189*, 2004.
- [7] J. L. Cardy. Boundary conditions, fusion rules and the verlinde formula. *Nuclear Physics B*, 324(3):581–596, 1989.
- [8] A. Chodos, R. Jaffe, K. Johnson, and C. B. Thorn. Baryon structure in the bag theory. *Physical Review D*, 10(8):2599, 1974.
- [9] A. Dei and L. Eberhardt. Correlators of the symmetric product orbifold. *Journal of High Energy Physics*, 2020(1):1–47, 2020.
- [10] R. Dijkgraaf, G. Moore, E. Verlinde, and H. Verlinde. Elliptic genera of symmetric products and second quantized strings. *Communications in Mathematical Physics*, 185(1):197–209, 1997.

BIBLIOGRAPHY

- [11] P. Francesco, P. Mathieu, and D. Sénéchal. *Conformal field theory*. Springer Science & Business Media, 2012.
- [12] J.-N. Fuchs and M. O. Goerbig. Introduction to the physical properties of graphene. *Lecture notes*, 10:11–12, 2008.
- [13] M. Fujita, K. Wakabayashi, K. Nakada, and K. Kusakabe. Peculiar localized state at zigzag graphite edge. *Journal of the Physical Society of Japan*, 65(7):1920–1923, 1996.
- [14] V. Gusynin, S. Sharapov, and J. Carbotte. Ac conductivity of graphene: from tight-binding model to 2+ 1-dimensional quantum electrodynamics. *International Journal of Modern Physics B*, 21(27):4611–4658, 2007.
- [15] F. D. M. Haldane. Model for a quantum hall effect without landau levels: Condensed-matter realization of the” parity anomaly”. *Physical review letters*, 61(18):2015, 1988.
- [16] I. Heemskerk, J. Penedones, J. Polchinski, and J. Sully. Holography from conformal field theory. *Journal of High Energy Physics*, 2009(10):079, 2009.
- [17] N. Ishibashi. The boundary and crosscap states in conformal field theories. *Modern Physics Letters A*, 4(03):251–264, 1989.
- [18] R. Jackiw and C. Rebbi. Solitons with fermion number 1/2. *Physical Review D*, 13(12):3398, 1976.
- [19] A. Karch, Z.-X. Luo, and H.-Y. Sun. Holographic duality for ising cft with boundary. *arXiv preprint arXiv:2012.02067*, 2020.
- [20] H. Karimi and I. Affleck. Towards a rigorous proof of magnetism on the edges of graphene nanoribbons. *Physical Review B*, 86(11):115446, 2012.
- [21] C. A. Keller. Phase transitions in symmetric orbifold cfts and universality. *Journal of High Energy Physics*, 2011(3):1–25, 2011.
- [22] A. Klemm and M. G. Schmidt. Orbifolds by cyclic permutations of tensor product conformal field theories. *Physics Letters B*, 245(1):53–58, 1990.

BIBLIOGRAPHY

- [23] J. Maldacena. The large- n limit of superconformal field theories and supergravity. *International journal of theoretical physics*, 38(4):1113–1133, 1999.
- [24] D. M. McAvity and H. Osborn. Conformal field theories near a boundary in general dimensions. *Nuclear Physics B*, 455(3):522–576, 1995.
- [25] G. Mussardo. *Statistical Field Theory: An Introduction to Exactly Solved Models in Statistical Physics*. Oxford University Press, 2020.
- [26] M. Nakahara. *Geometry, topology and physics*. CRC press, 2018.
- [27] A. C. Neto, F. Guinea, N. M. Peres, K. S. Novoselov, and A. K. Geim. The electronic properties of graphene. *Reviews of modern physics*, 81(1):109, 2009.
- [28] A. J. Niemi and G. W. Semenoff. Axial-anomaly-induced fermion fractionization and effective gauge-theory actions in odd-dimensional space-times. *Physical Review Letters*, 51(23):2077, 1983.
- [29] A. J. Niemi and G. W. Semenoff. Fermion number fractionization in quantum field theory. *Physics Reports*, 135(3):99–193, 1986.
- [30] A. Recknagel. Permutation branes. *Journal of High Energy Physics*, 2003(04):041, 2003.
- [31] K. Roumpedakis. Comments on the sn orbifold cft in the large n -limit. *Journal of High Energy Physics*, 2018(7):1–22, 2018.
- [32] M. Sato, Y. Takahashi, and S. Fujimoto. Non-abelian topological order in s-wave superfluids of ultracold fermionic atoms. *Physical review letters*, 103(2):020401, 2009.
- [33] G. W. Semenoff. Condensed-matter simulation of a three-dimensional anomaly. *Physical Review Letters*, 53(26):2449, 1984.
- [34] G. W. Semenoff. Engineering holographic graphene. In *AIP Conference Proceedings*, volume 1483, pages 305–329. American Institute of Physics, 2012.

- [35] G. W. Semenoff and F. Zhou. Magnetic catalysis and quantum hall ferromagnetism in weakly coupled graphene. *Journal of High Energy Physics*, 2011(7):1–28, 2011.
- [36] T. Takayanagi. Holographic dual of a boundary conformal field theory. *Physical review letters*, 107(10):101602, 2011.
- [37] E. Verlinde. Fusion rules and modular transformations in 2d conformal field theory. *Nuclear Physics B*, 300:360–376, 1988.

Appendix A

Useful Relations in Complex Coordinates

We have defined our complex coordinates as $z = x^0 + ix^1$, $\bar{z} = x^0 - ix^1$. Inverting, $x^0 = \frac{1}{2}(z + \bar{z})$, $x^1 = -\frac{i}{2}(z - \bar{z})$. First, let's derive the vector transformation law. To do this, we further define the notation $x^z \equiv z$, $x^{\bar{z}} \equiv \bar{z}$. Now, a vector transforms as

$$V_\mu = \frac{\partial x^\alpha}{\partial x^\mu} V_\alpha \quad (\text{A.1})$$

This gives

$$V_z = \frac{\partial x^0}{\partial x^z} V_0 + \frac{\partial x^1}{\partial x^z} V_1 = \frac{1}{2}(V_0 - iV_1). \quad (\text{A.2})$$

Similarly, $V_{\bar{z}} = \frac{1}{2}(V_0 + iV_1)$. Inverting,

$$V_0 = V_z + V_{\bar{z}}, \quad V_1 = i(V_z - V_{\bar{z}}). \quad (\text{A.3})$$

Similarly the transformation law for a general tensor $T_{\mu_1\mu_2\dots\mu_n}$ can be derived.